

# Journal of Materials Chemistry C

Accepted Manuscript



This is an *Accepted Manuscript*, which has been through the Royal Society of Chemistry peer review process and has been accepted for publication.

*Accepted Manuscripts* are published online shortly after acceptance, before technical editing, formatting and proof reading. Using this free service, authors can make their results available to the community, in citable form, before we publish the edited article. We will replace this *Accepted Manuscript* with the edited and formatted *Advance Article* as soon as it is available.

You can find more information about *Accepted Manuscripts* in the [Information for Authors](#).

Please note that technical editing may introduce minor changes to the text and/or graphics, which may alter content. The journal's standard [Terms & Conditions](#) and the [Ethical guidelines](#) still apply. In no event shall the Royal Society of Chemistry be held responsible for any errors or omissions in this *Accepted Manuscript* or any consequences arising from the use of any information it contains.

Cite this: DOI: 10.1039/c0xx00000x

www.rsc.org/xxxxxx

## FEATURE ARTICLE

**Application of singlet energy transfer in triplet state formation: broadband visible light-absorbing triplet photosensitizers, molecular structure design, related photophysics and applications**

Xiaoneng Cui, Caishun Zhang and Kejing Xu and Jianzhang Zhao\*

5 Received (in XXX, XXX) Xth XXXXXXXXXX 20XX, Accepted Xth XXXXXXXXXX 20XX

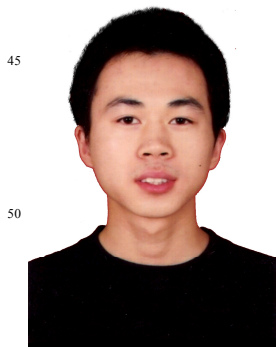
DOI: 10.1039/b000000x

Conventional triplet photosensitizers usually contain a single visible light-harvesting chromophore, which is responsible for the dual-functionality of light-harvesting and intersystem crossing (ISC). These profiles render a few disadvantages, such as a single absorption band in the visible spectral range, low efficiency of harvesting broadband visible light (e.g. solar light); and it is difficult to design new triplet photosensitizers because the relation between molecular structure and ISC is unclear. In order to address these challenges, application of the Förster-Resonance-Energy-Transfer (FRET) and spin converter lead to a new molecular structure profile for triplet photosensitizers to attain the broadband visible light-absorption, and disintegrated functionality of visible light-harvesting and ISC. This review article summarized the triplet photosensitizers showing broadband visible light absorption, include the molecular design rationales, the photophysical processes involved in these photosensitizers, such as the FRET, ISC, the photo-induced electron transfer (PET) studied with nanosecond and femtosecond transient absorption spectroscopies. The application of the triplet photosensitizers in photoredox catalytic organic reactions and triplet-triplet annihilation upconversion were also discussed. We summarized the molecular structure-property relationship of these new photosensitizers, as well as the challenges in this emerging area.

**1. Introduction**

Triplet photosensitizers are versatile compounds which have been widely used in photodynamic therapy (PDT),<sup>1-8</sup> catalytic hydrogen (H<sub>2</sub>) production,<sup>9-12</sup> and photoredox catalytic organic reactions,<sup>13-17</sup> phosphorescent biological imaging,<sup>18-22</sup> molecular logic gates,<sup>23,24</sup> and more recently the triplet-triplet-annihilation (TTA) upconversion.<sup>25-30</sup> Triplet photosensitizers are compounds with triplet excited state efficiently populated upon photoexcitation, via intersystem crossing (ISC). Different from the application of *singlet* excited state, for which *fluorescence* is

very often the purpose,<sup>31-33</sup> the application of the *triplet* excited state of the triplet photosensitizers is usually to initiate *intermolecular electron transfer* or *triplet-triplet-energy-transfer* (TTET).<sup>8</sup> Thus, the desired photophysical property of the triplet photosensitizers include strong absorption of visible light, high triplet state yields and long triplet excited state lifetimes.<sup>8</sup> These properties exert significant influence on the performance of the triplet photosensitizers in the areas such as photocatalysis, and TTA upconversion. This scenario is different from that of the applications for which strong absorption of visible light is unnecessary, such as electroluminescence. Moreover,



Xiaoneng Cui received his B. S. degree in Material Chemistry from AnQing Normal University in 2011. Since 2011 he has been a Ph.D. student in Prof. J. Zhao's group, at Dalian University of Technology. Currently his research interests mainly focus on organic chromophores that show strong absorption of visible light and long-lived triplet excited states and exploring their applications for switching of triplet-triplet annihilation (TTA) upconversion and photooxidation.



Caishun Zhang obtained his bachelor's degree in Liaoning Normal University in June 2008. After that, in June 2011, he obtained his master degree in Liaoning Normal University. Currently, he is a PhD student in the group of Professor Jianzhang Zhao, Dalian University of Technology. His research interest includes intramolecular RET enhanced visible light absorbing organic triplet photosensitizers and TTA annihilation upconversion.

triplet excited state lifetime of the electroluminescent materials must be *short* to avoid the saturation effect.<sup>34–39</sup> Thus, the designing of the triplet photosensitizers is complicated by the above mentioned requirements, it may follow different rules of that for the electroluminescent materials, such as strong absorption of visible light and long-lived triplet excited state. Another major challenge in study of triplet photosensitizer is the difficulties in molecular structural designing of new triplet photosensitizers, especially to attain broadband visible light absorption.<sup>8</sup> In the following section we will discuss the reasons for these prerequisite of the photophysical properties of triplet photosensitizers.

The desired photophysical property of strong absorption of visible light ( $\epsilon$ ), high triplet state yield ( $\Phi_T$ ) and long triplet state lifetime ( $\tau_T$ ) can be rationalized as following, exemplified with the TTET. The efficiency of the TTET can be evaluated quantitatively by the Stern-Volmer quenching of the triplet state of the energy donor by the triplet energy acceptor (the quencher), by Eq. 1.<sup>40</sup>

$$\frac{\tau_0}{\tau} = 1 + K_{SV}[Q] \quad (\text{Eq. 1})$$

where  $\tau_0$  is the triplet state lifetime of the triplet photosensitizer,  $\tau$  is the quenched triplet state lifetime of the triplet photosensitizer in the presence of triplet acceptor.  $[Q]$  is the concentration of the quencher (triplet energy acceptor), and  $K_{SV}$  is the Stern-Volmer constants. The larger the constant, the more efficient quenching (TTET) will be resulted. The  $K_{SV}$  can be broken down to Eq. 2:

$$K_{SV} = k_q \tau_0 \quad (\text{Eq. 2})$$

where  $k_q$  is the bimolecular quenching constants, and  $\tau_0$  is the intrinsic triplet state lifetime of the triplet photosensitizer.  $k_q$  is a value smaller than the diffusion controlled bimolecular collision constant ( $k_0$ ). In fluid solution, the  $k_q$  is a value close to  $k_0$ ,  $f_Q$  is a value smaller than 1:

$$k_q = f_Q \times k_0 \quad (\text{Eq. 3})$$

$k_0$  is a value defined by Eq. 4 and Eq. 5

$$k_0 = 4\pi RND/1000 = \frac{4\pi N}{1000} (R_f + R_q)(D_f + D_q) \quad (\text{Eq. 4})$$

$$D = kT/6\pi\eta R \quad (\text{Eq. 5})$$

As discussed above, the quenching efficiency, or the TTET efficiency, is mainly dependent on the triplet state lifetime ( $\tau_T$ ) of the triplet photosensitizer. Long triplet state lifetime is beneficial for efficient TTET. This postulation has been unambiguously confirmed by the application of triplet photosensitizers showing long triplet state lifetimes in TTA upconversion.<sup>41</sup> On the other hand, most of the TTET process, and the ‘concentration’ of the triplet energy acceptor at the triplet excited state, is directly proportional to the ‘concentration’ of the excited photosensitizer. Thus, the visible light absorption (molecular absorption coefficient,  $\epsilon$ ) of the triplet photosensitizer is also crucial.

Most of the known triplet photosensitizers usually show weak absorption of visible light, short triplet excited state lifetimes, and the molecular structures are difficult to be modified or rationally designed.<sup>2,3,8,41–43</sup> Recently we and other researchers developed new molecular structural designing approaches to address the above challenges (Fig. 1).<sup>8,43</sup> For example, in order to attain strong absorption of visible light and efficient conversion of the photoexcitation energy into the triplet state manifold, direct metalation of organic chromophore, or selection of ligands and coordination center with matching singlet energy levels to ensure efficient energy transfer were employed.<sup>8,44</sup> Iodo or bromo Bodipys were also developed as a novel class of organic triplet photosensitizers.<sup>5,8,45</sup> In order to design heavy atom-free organic triplet photosensitizers, spin converters, such as fullerene ( $C_{60}$ ), were used for ISC thus formation of triplet state.<sup>8,46–48</sup> Detail discussion of these molecular structure designing methods have been presented in a recent review.<sup>8</sup>

Despite of these achievements, there is still another major challenge in the designing of triplet photosensitizers for efficient harvesting of broadband excitation light, such as solar light. Conventional triplet photosensitizers are usually based on a single light-harvesting chromophore, as a result, these is only one major absorption band in visible spectral region.<sup>1–3</sup> The typical absorption spectra of a few triplet photosensitizers were presented in Fig. 2. For the mono-chromophore triplet photosensitizers, these is only *one* major absorption band in visible spectral region. Moreover, it is clear that the absorption of **9** in visible region is weak, and the absorption wavelength is only 450 nm ( $\epsilon < 20000 \text{ M}^{-1}\text{cm}^{-1}$ ). The weak transition of the  $S_0 \rightarrow {}^1\text{MLCT}$  can be attributed to the charge transfer (CT) character of the transition.<sup>49,42</sup> It should be noted that some Ru(II) complexes used for solar cells show longer absorption



Kejing Xu received his BS degree in applied chemistry from Anhui University of Science and Technology in 2012. Since 2012 he has been a PhD student in Prof. J. Zhao's group. His research focuses on switching of the property of triplet photosensitizers, as well as modulating triplet-triplet annihilation upconversion with optical or chemistry inputs.



Prof. Jianzhang Zhao received his Ph.D. degree in organic chemistry from Jilin University in 2000. After postdoctoral research at Pohang University of Science and Technology (South Korea), Max Planck Research Unit for Enzymology of Protein Folding (Germany) and University of Bath (UK) from 2000 to 2005, he returned to China to take his current position. His research interests include synthetic chemistry, photochemistry, photophysics and computation chemistry.

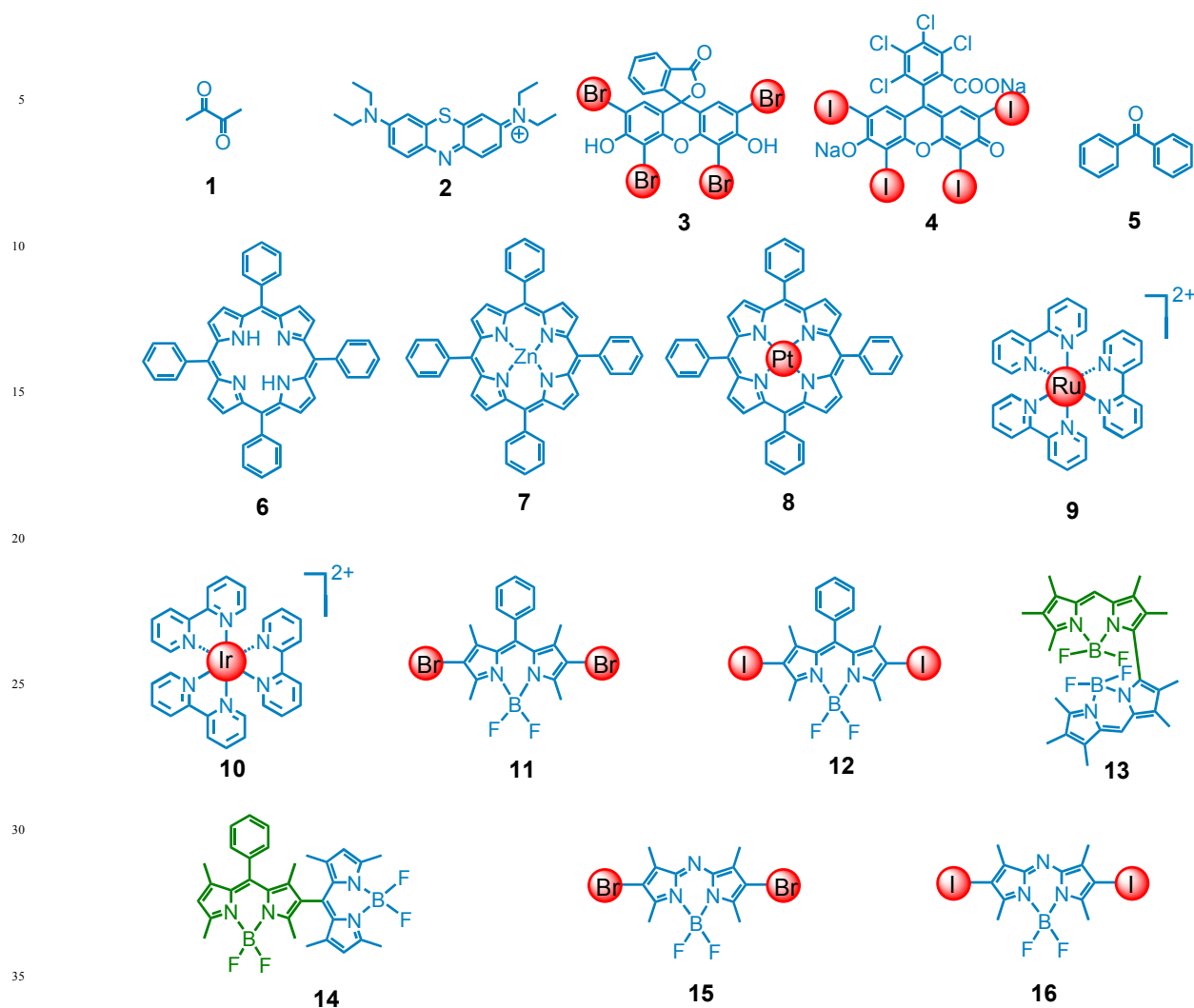
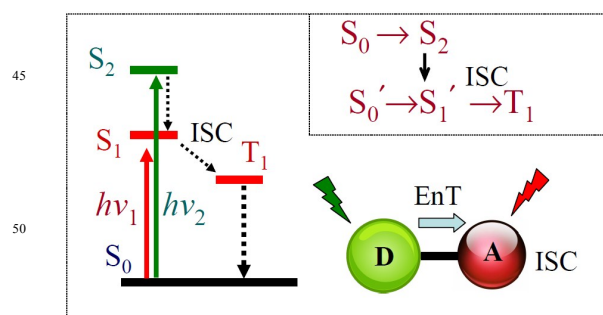


**Fig. 1** The typical triplet photosensitizers, most are based on mono light-harvesting chromophore profile.

wavelength and large  $\epsilon$  values, however, the lifetime of the triplet excited states of these Ru(II) complexes are usually too short to ensure efficient intermolecular energy transfer.<sup>49,50</sup>

Concerning the application of the triplet photosensitizers, the conventional application is photodynamic therapy (PDT) studies.<sup>1-3</sup> Recently new areas were developed, such as photoredox catalytic organic reactions,<sup>13</sup> and TTA upconversion.<sup>26,28-30</sup> Most of the photocatalysts used in the photoredox catalytic organic reactions are the conventional



**Scheme 1** A simple schematic diagram for molecular design rationales of RET enhanced broadband visible light-harvesting triplet photosensitizers. RET stands for Resonance-Energy-Transfer, ISC stands for intersystem crossing, and EnT stands for energy transfer. D stands for energy donor and A stands for energy acceptor. Photoinduced electron transfer between the energy donor and the acceptor was omitted for clarity.

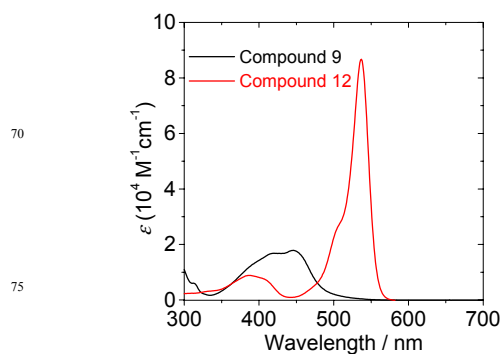


**Fig. 2** UV-vis absorption spectra of compounds (a) 9 and (b) 12.

compounds, such as **3**, **4**,<sup>53,54,55</sup> **9**<sup>51</sup> and **10**.<sup>52</sup> More efficient triplet photosensitizers are desired for these applications, such as those triplet photosensitizers showing strong absorption of visible light and long-lived lifetime of triplet excited states

In order to attain broadband visible light absorption, multichromophore dyads and triads triplet photosensitizers can be designed, based on fluorescence-resonance-energy-transfer (FRET) and spin converter for triplet state formation (Scheme 1).<sup>8,56–58</sup> The photophysical processes of the FRET/spin converter based energy funneling broadband visible light-harvesting triplet photosensitizers are as following. Two (or more) different chromophores are linked together, via covalent bond or supramolecular interactions. Each of the chromophores show strong absorption of visible light, but at different wavelength. The FRET energy donor will transfer the photoexcitation energy to the energy acceptor. The FRET energy acceptor is with ISC capability, thus the funneled photoexcitation energy is able to be efficiently transformed to the energy of triplet excited state. Thus triplet photosensitizers showing broadband visible light-absorption are obtained.<sup>8</sup>

It should be pointed out that FRET was widely used in *singlet* excited state-related compounds, such as fluorescent molecular arrays as light-absorbing antenna.<sup>59–63</sup> However, this method was rarely used for production of triplet excited state upon excitation with broadband light source, such as solar light. This area witnessed significant progress in the past few years,<sup>48,56–58,64</sup> and the application of these broadband visible light-absorbing triplet photosensitizers in photocatalysis and TTA upconversion is promising.<sup>58,64</sup> This review will focus on introduction of these triplet photosensitizers, include the molecular designing rationales, the photophysical processes and the applications. Some of the photophysical processes involved in these multichromophore triplet photosensitizers are unique, for example, ping-pong energy transfer (forward singlet energy transfer and backward triplet energy transfer),<sup>65</sup> and excited states equilibrium.<sup>56</sup> These photophysical processes will be introduced with specific exemplars. The detail of the FRET mechanism was well established previously,<sup>40</sup> and will not be discussed herein.

It should be pointed out that the alternative approach, i.e. to construct broadband visible light-absorbing triplet photosensitizers (dyads) by linking two triplet photosensitizers was not studied. In this case intramolecular TTET will occur, and the triplet state will localize on one part of the dyad. This approach may be more synthetically demanding than the above mentioned FRET/ISC approach with only one part as spin converter.

## 2. Broadband visible light-absorbing multi-chromophore conjugates for triplet state formation

### 2.1. Covalent bond linked Bodipy-porphyrin conjugations

In 1998 Lindsey studied the energy transfer in Bodipy-porphyrin light-harvesting array **17–21** (Fig. 3).<sup>66</sup> The linker between the Bodipy and the porphyrin moieties is rigid. Based on different structural profile (Fig. 3), different number of Bodipy antenna can be attached to the porphyrin core. There is no  $\pi$ -conjugation between the Bodipy and porphyrin moieties, otherwise the molecule is no longer a supramolecular system, and the excited

states collapsed into that of one chromophore, no significant broadband absorption can be resulted.

The Soret band of porphyrin is strong (419 nm), the absorbance at longer wavelength, e.g. 514 nm, however, is only 5% of the absorbance at 419 nm (Fig. 4). Bodipy shows strong absorption at 516 nm, which is complementary to the absorption of porphyrin. Bodipy antenna can be attached at the para position of the phenyl ring on the porphyrin, thus more Bodipy antenna can be introduced to the molecule.

The Bodipy moieties in **17–21** show low fluorescence quantum yields ( $\Phi_F = 5\%$ ), which is much lower than the parent Bodipy without any substituents on the meso position ( $\Phi_F = 30–80\%$ ).<sup>59,61</sup> The low fluorescence quantum yields of the Bodipy building blocks in the conjugates **17–21** is actually due to the free rotor effect of the phenyl ring at the meso position of the Bodipy chromophore,<sup>67</sup> a property was later utilized to develop fluorescent viscosity molecular sensors.<sup>68,69</sup> As a proof, introducing methyl substituent at 1,7-position of the Bodipy core increase the fluorescence quantum yield dramatically, because the free rotation of the phenyl ring is hindered.<sup>1,32,70–73</sup>

The decay of the singlet excited state of the Bodipy moieties in **17**, **18**, **20**, **21** is faster than the normal Bodipy derivative showing high fluorescence quantum yield. Biexponential decay of the singlet excited state were found for the Bodipy building block in the conjugates in **17–21**, as 15 ps and 500 ps, which are assigned to the singlet excited states with different conformations (generated by the different dihedral angles between the Bodipy core and the 5-phenyl ring). It should be pointed out that using of such Bodipy building blocks, rather than the Bodipy units with methyl groups at 1,7-position to hinder the free rotation of the phenyl ring at the meso position,<sup>1,32,71</sup> is probably detrimental to the light harvesting effect, due to the fast non-radiative decay of the singlet excited states of the antenna, a process which is competitive to the FRET process (may take a few ps or even longer time).<sup>62</sup> Fortunately, the FRET in the Bodipy-porphyrin conjugates (Fig. 3) is fast. The decay of the Bodipy unit become much faster in the arrays (2 and 20 ps, respectively). This time scale can be treated as the rate of FRET.

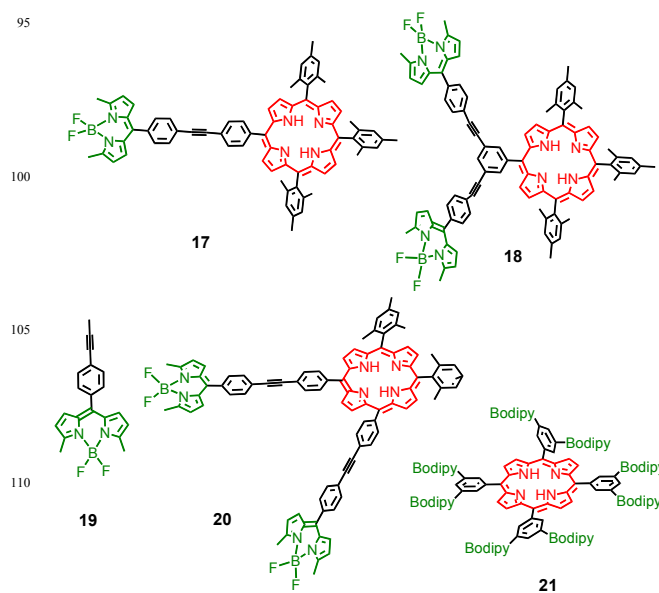


**Fig. 3** Light-harvesting molecular arrays comprised of porphyrin and Bodipy antenna (Bodipy = **19**).<sup>66</sup>

Base on the steady state and the femtosecond time-resolved transient absorption spectroscopy, it was proposed that the energy transfer mechanism is mainly the through-bond-energy-transfer (TBET).<sup>74,75</sup> This conclusion is derived from the following considerations. The rates of energy transfer are essentially the same for arrays in which the connections of the Bodipy unit are at the meta-versus para-position on the meso-aryl ring of the linker to the porphyrin core. If the Förster through-space mechanism exclusively applied for the energy transfer in the conjugates, observable differences in the energy-transfer rates and efficiencies for the different architectures would be expected. However, such differences in the FRET kinetics were not observed.

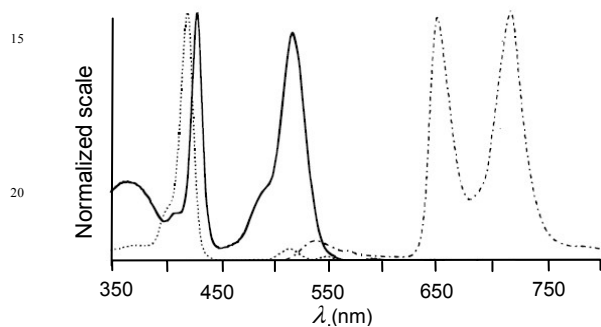


**Fig. 4** Overlay of the absorption spectrum of FbTPP (dashed line. Fb = free base) with the absorption spectrum (solid line) and the fluorescence emission spectrum (dot-dashed line) of **17** obtained upon illumination at 485 nm (toluene, 298 K). Reproduced with permission from Li et al.<sup>66</sup>

The free base of porphyrin actually show efficient ISC ( $\Phi_T = 90\%$ ).<sup>76,77</sup> Thus, following the funneling of the photoexcitation energy from the Bodipy antenna to the porphyrin core of the molecular conjugates (Fig. 3), triplet excited state may be produced via the ISC of the porphyrin moiety, given the process is not inhibited by any photo-induced electron transfer (PET), or charge separation (CS).<sup>78,79</sup> However, the photophysical property of the Bodipy-porphyrin arrays was not studied with the nanosecond transient absorption spectroscopy, or singlet oxygen ( $^1O_2$ ) photosensitizing experiments.<sup>66</sup> Thus no information concerning the triplet excited state of the array was presented.<sup>66</sup> It should be pointed out the femtosecond transient absorption spectrometer is not suitable for study of the triplet excited state, which are usually with much longer lifetimes than the singlet excited states, due to the limitation of the optical delay line in the femtosecond transient absorption spectrometer (only for a few ns).

## 2.2. Bodipy-tetraphenyltetraazaporphyrin conjugates

In 2011, Thompson et al reported the Bodipy-tetraphenyltetraazaporphyrin (TPBP) Pt(II) bichromophoric complex (**22**) (Fig. 5).<sup>65</sup> The designing of this molecular is with a clear goal, i.e. to prepare a broadband visible light-absorbing triplet photosensitizer, based on the energy transfer between Bodipy chromophores and the benzoporphyrin-Pt coordination center. It should be pointed out that the fast non-radiative decay channel still exist for the Bodipy chromophore selected for the conjugates (Fig. 5). However, as discussed earlier, this fast decay channel does not necessarily mean an inhibition of FRET effect, given the latter (FRET process) is faster.

The absorption of the Bodipy moiety is complementary to the

absorption of complex **24**, i.e. the Bodipy moiety shows strong absorption at 514 nm (Fig. 6). With four Bodipy antenna, the complex shows an absorption at 514 nm which is comparable to the Soret band of the complex **24** at ca. 425 nm. Phosphorescence at 770 nm was observed, which is attributed to the Pt(II) coordination center, and Bodipy units do not contribute directly to the phosphorescence emission.

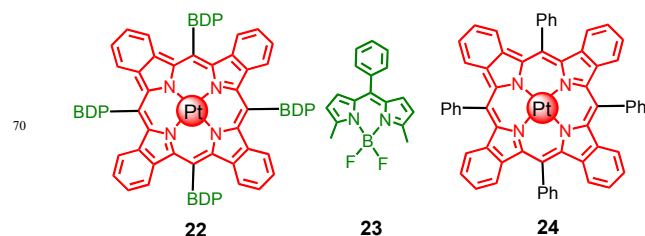


**Fig. 5** The broadband visible light-harvesting Bodipy-tetraphenyltetraazaporphyrin complex (**22**). The Bodipy chromophore (**23**) and the unsubstituted Pt(TPBP) complex (**24**) were also presented.<sup>65</sup>

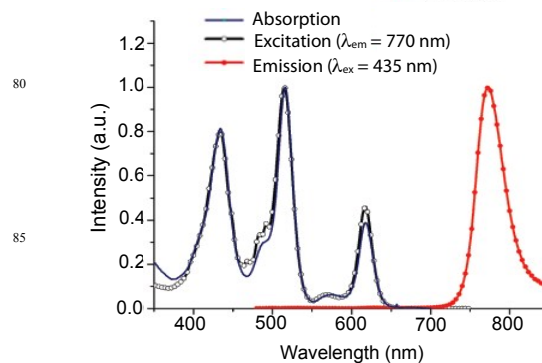


**Fig. 6** Normalized absorption, excitation ( $\lambda_{em} = 770$  nm), and emission ( $\lambda_{ex} = 435$  nm) spectra of complex (**22**) in toluene. Reproduced with permission from Whited et al.<sup>65</sup>

The phosphorescence excitation spectrum demonstrated the efficient singlet energy transfer from the Bodipy moiety to the Pt(II) coordination center (Fig. 6).<sup>80</sup> The phosphorescence lifetime of the complex is 67  $\mu$ s, which is much longer than the unsubstituted complex **24** (30  $\mu$ s). Thus the Bodipy chromophore exerted substantial influence on the excited state of the complex **24**.

The ultrafast transient absorption spectrum of the complex was recorded upon selective photoexcitation into the Bodipy part (Fig. 7. 10–200 ps delay). Upon femtosecond pulsed laser excitation, bleaching band at 515 nm were observed, which is due to the depletion of the ground state of the Bodipy moiety. At the same time, bleaching bands at 450 nm and 620 nm were also observed, which are due to the depletion of the ground state of the coordination center of complex **22**. With longer delay, the bleaching band at 515 nm diminished, while the bleaching bands at 450 nm and 620 nm grows over ca. 10 ps. Thus singlet energy transfer in the complex **22** was confirmed. Fitting the curves give a singlet energy transfer time of  $1/k_{EnT} = 1.29 \pm 0.11$  ps.

After 10 ps, the transient spectrum is identical to the triplet state of complex **22** (Fig. 8), because it was shown the ISC of the complex **24** takes only about 400 fs. Therefore the singlet excited

state of the Pt(II) coordination center won't be accumulated, due to the fast draining channel of ISC. At longer delay time, however, the bleaching bands at 450 nm and 620 nm diminished, and the bleaching band at 515 nm grows in Fig. 8. These changes indicated the backward triplet-triplet-energy transfer (TTET) from the Pt(TPBP) coordination center to the Bodipy moiety. The rate constant is  $k_{\text{TTET}} = 1.0 \times 10^{10} \text{ s}^{-1}$ . It should be pointed out that this kind of ping-pong energy transfer, i.e. forward singlet energy transfer and the backward triplet energy transfer, was not observed with the fluorescent FRET molecules.<sup>62,81–84</sup>

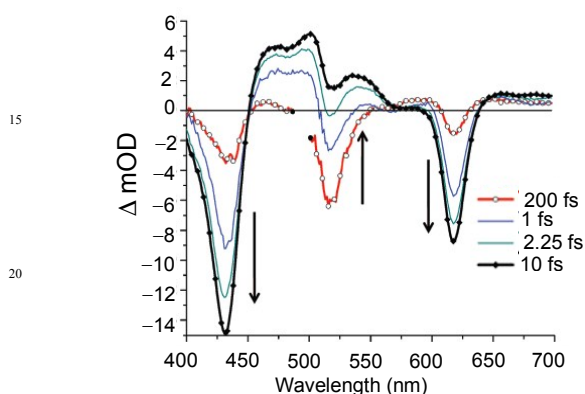


Fig. 7 Ultrafast transient absorption spectra of **22** in toluene after excitation at 508 nm (0.2–10 ps). Reproduced with permission from Whited et al.<sup>65</sup>

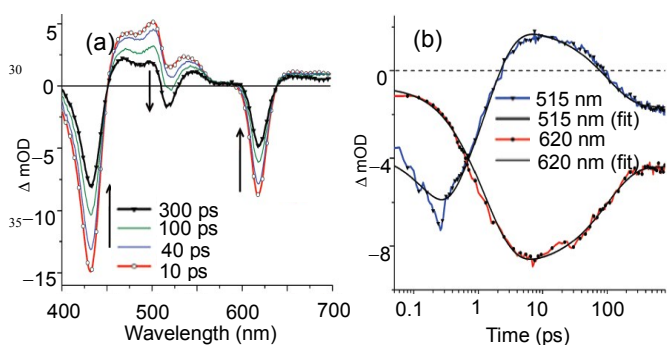


Fig. 8 (a) Ultrafast transient absorption spectra of **22** after excitation at 508 nm (10–300 ps). (b) Transient absorptions at 515 nm (BODIPY) and 620 nm (porphyrin) with predicted traces based on kinetic parameters for the system. Reproduced with permission from Whited et al.<sup>65</sup>

Nanosecond transient absorption spectroscopy of complex **22** was studied.<sup>65</sup> Three bleaching bands at 430 nm, 515 nm, 620 nm were observed promptly upon nanosecond pulsed laser excitation. These bleaching bands indicated the triplet state is delocalized on the Bodipy and the Pt(TBTP) moieties, in other words, there is triplet state equilibrium in conjugate **22**. All the transient signals in the spectra decay with the same kinetics, the triplet state lifetime (and the phosphorescence lifetime) is 67  $\mu\text{s}$ , which is much longer than the 30  $\mu\text{s}$  lifetime of the unsubstituted complex **24**. This extension of the triplet state lifetime is attributed to the energy reservoir effect of the Bodipy chromophore.<sup>65</sup>

The photophysical processes of complex **22** is summarized in Fig. 9. Selective photoexcitation of the Bodipy antenna by 510 nm pump produces the singlet excited state of Bodipy. Then the FRET will lead to the formation of the singlet excited state of

Pt(TPBP) moiety. The ultrafast ISC of Pt(TPBP) moiety produce the triplet excited state of the Pt(TPBP) moiety. Then the TTET produce the triplet state of Bodipy, and a triplet state equilibrium was established. Based on the relationship between the TTET rate constant and the number of the intervening phenylene units, the authors propose the TTET is a phenylene linker-mediated superexchange mechanism.

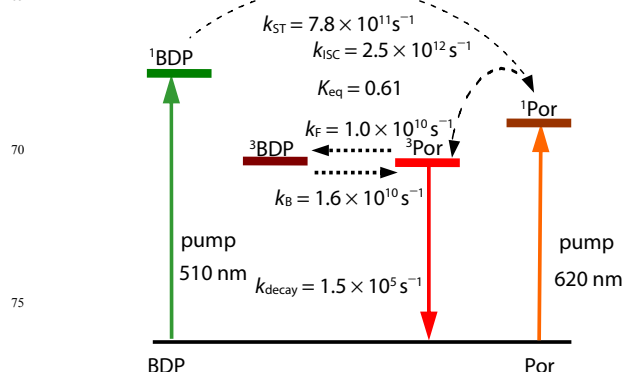


Fig. 9 Jablonski diagram summarizing the excited-state behaviour of complex **22** upon selective photoexcitation into the BODIPY or benzoporphyrin units. Reproduced with permission from Whited et al.<sup>65</sup>

### 2.3. Bodipy-containing Pt(II)(diimine)(dithiolate) complexes

As a typical photophysical feature, the visible light-absorption of normal triplet photosensitizers is actually weak.<sup>8</sup> For example, Pt(II)(diimine)(dithiolate) complexes have been demonstrated to be able to inject electron into titanium oxide, thus the complexes are useful for photovoltaics. These complexes have also been used in photocatalytic hydrogen ( $\text{H}_2$ ) production. However, these complexes show only moderate absorption of visible light at ca. 550 nm ( $\epsilon < 10^4 \text{ M}^{-1} \text{ cm}^{-1}$ ), which is at least one order of scale smaller than the typical organic dyes such as Bodipy, which show absorption in visible spectral region with  $\epsilon$  value up to  $8 \times 10^4 \text{ M}^{-1} \text{ cm}^{-1}$ .<sup>1,70,85</sup>

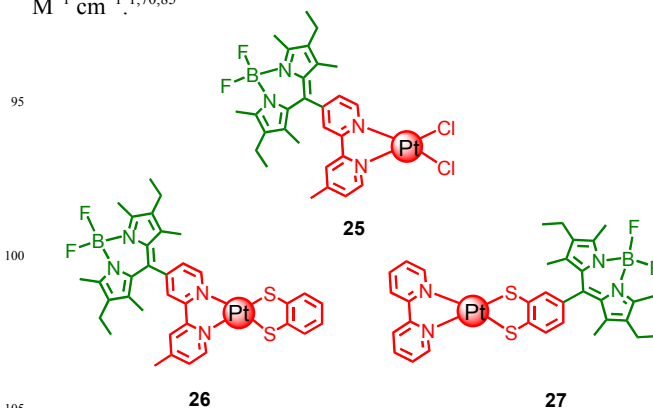
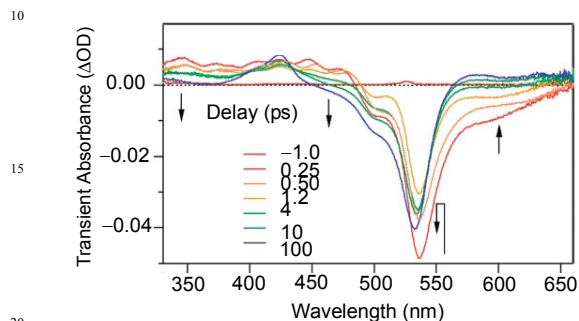


Fig. 10 Bodipy-Pt(II)(diimine)(dithiolate) dyads (**25** – **27**) showing strong absorption of visible light.<sup>86</sup>

Eisenberg et al used Bodipy ligand to preparation of Pt(II) diimide(dithiolate) complexes (Fig. 10). The Bodipy chromophore is either attached on the bipyridine ligand (complexes **25** and **26**), or on the dithiolate ligand (complex **27**).<sup>86</sup> The Bodipy moiety shows absorption at 527 nm (with  $\epsilon = 70000 \text{ M}^{-1} \text{ cm}^{-1}$ ), and the Pt(II) coordination center shows absorption band at ca. 600 nm ( $\epsilon = 8000 \text{ M}^{-1} \text{ cm}^{-1}$ ). Both the

UV-vis absorption and the electrochemical data infer that the property of the dyads **26** and **27** are the sum of the components of the dyads, thus there is no significant electronic interaction between the components in the dyads at ground state. Interestingly, both the mixed-metal-ligand-to-ligand' charge transfer (MMLL'CT) emission of the Pt(II) coordination center and the Bodipy fluorescence were quenched, which indicated either energy transfer, or electron transfer.



**Fig. 11** Femtosecond transient absorption spectra for **26** obtained with a 530 nm pump pulse. The 530 nm excitation directly excites the  $^1\pi\pi^*$  absorption band of the Bodipy moiety. Reproduced with permission from Lazarides et al.<sup>86</sup>

Femtosecond transient absorption spectra of the complex **26** was recorded to reveal the photophysical processes (Fig. 11). Upon selective excitation into the Bodipy ligand (530 nm), the spectra show the ground state bleaching band of Bodipy moiety at 530 nm, and the stimulated emission (SE) band at ca. 600 nm. The ground state bleaching band decrease significantly within 2 ps, with decrease of the excited state absorption (ESA) at 350 nm. This process is the  $^1\text{Bodipy} \rightarrow ^1\text{MMLL'CT}$  singlet energy transfer process. The bleaching basically did not change during the following 2–6 ps, during which the ISC of  $^1\text{MMLL'CT} \rightarrow ^3\text{MMLL'CT}$  took places. Then the bleaching band increased again, with the increasing of the ESA at 425 nm (which is the featured ESA of the Bodipy triplet state), the process takes 6–8 ps (Fig. 12), which is attributed to the  $^3\text{MMLL'CT} \rightarrow ^3\text{Bodipy}$  TTET process.

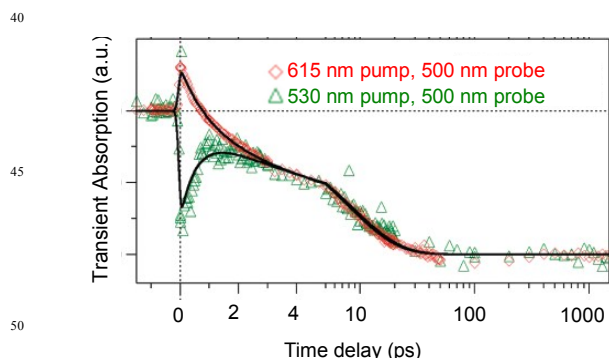


**Fig. 12** Kinetics of **26** at probe wavelengths of 500 and 489 nm, following excitation at 530 (green symbols) or 600 or 615 nm (red symbols). The kinetics at these probe wavelength are indicative of the bleach of the Bodipy  $\pi\pi^*$  absorption band. Reproduced with permission from Lazarides et al.<sup>86</sup>

The photophysical processes of **26** can be summarized in Fig. 13. Upon selective photoexcitation into the  $^1\text{Bodipy}$  singlet excited state, the singlet energy transfer takes place, which lead

to the formation of MMLL'CT singlet excited state. The ultrafast ISC ( $<1$  ps) of the Pt(II) coordination center produces the triplet excited state ( $^3\text{MMLL'CT}$ ). Then the intramolecular TTET leads to the formation of the triplet excited state of Bodipy. Based on these photophysical processes, both the fluorescence of the Bodipy moiety and the phosphorescence of Pt(II) coordination center should be quenched, which is in agreement with the experimental results.

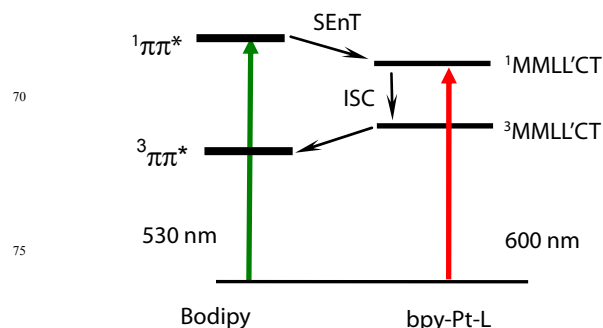


**Fig. 13** Energy level diagram relevant to the photochemistry of complex **26** and **27**. Reproduced with permission from Lazarides et al.<sup>86</sup>

Analysis of the spectral overlap and the dipole moments orientation in dyad **26** predict a slow singlet energy transfer (710 ps). However, the experimental value for the singlet energy transfer time is 0.6 ps. Thus it was proposed that electron exchange is responsible for the ultrafast singlet energy transfer in **26**, not the Förster mechanism (FRET). Moreover, it was proposed the electron exchange play the major rule for the triplet energy transfer. However, the triplet excited state lifetime of the complexes **26** and **27** were not disclosed.

Concerning of visible light-harvesting and formation of triplet excited state, the designing of the molecular structures of dyads **26** and **27** is successful to large extent. However, the triplet excited state is no longer localized on the Pt(II) coordination center, rather, it is re-located to the Bodipy moiety, which may change the excited state redox property, thus the photocatalysis may be affected.

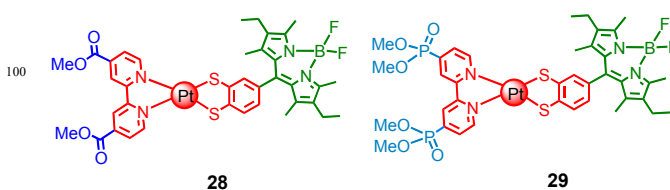


**Fig. 14** Pt(II) dimine dithiolate complex (**28**, **29**) containing Bodipy antenna. The mixed-metal-ligand-to-ligand' charge transfer ( $^3\text{MMLL'CT}$ ) state is with lower energy level than the Bodipy triplet excited state.<sup>87</sup>

To address this problem, the same group modified the molecular structure, electron withdrawal groups were attached on the bpy ligand, thus the energy level of the mixed-metal-ligand-to-ligand' charge transfer ( $^3\text{MMLL'CT}$ ) state become lower than that of the Bodipy triplet state, thus the  $T_1$  state of the dyads **28** and **29** is localized on the Pt(II) coordination center, not on Bodipy antenna.<sup>87</sup> This tuning of the confinement of the excited state may be beneficial to the catalytic activity.

#### 2.4. Bodipy-Porphyrin conjugates with C<sub>60</sub> as electron acceptor

In multichromophore conjugates, besides the desired energy transfer, electron transfer is very often the process involved. In some cases the formation of triplet excited state can be inhibited by formation of charge transfer state (CTS). However, in some cases the charge recombination (CR) may produce the triplet state.<sup>88</sup>

A representative charge separation Bodipy-Porphyrin-C<sub>60</sub> pentad (**30**) was reported.<sup>89</sup> The Bodipy antenna shows absorption at 504 nm, and the Zn porphyrin coordination center gives absorption at 434 nm. The emission of the Bodipy antenna in compound **31** was quenched as compared with that of the free Bodipy. Moreover, the fluorescence of the Zn(II) porphyrin coordination center was not quenched, and the fluorescence excitation spectrum of **7** shows a band at ca. 504 nm, therefore singlet energy transfer was confirmed for **31**, with Bodipy as the singlet energy donor and the Zn(II) porphyrin coordination center as the singlet energy acceptor. For pentad **30**, however, the fluorescence of the Zn(II) porphyrin coordination moiety was quenched, and no fluorescence of the C<sub>60</sub> moiety was observed (expected to be at 720 nm). Thus, PET was proposed for pentad **30**.

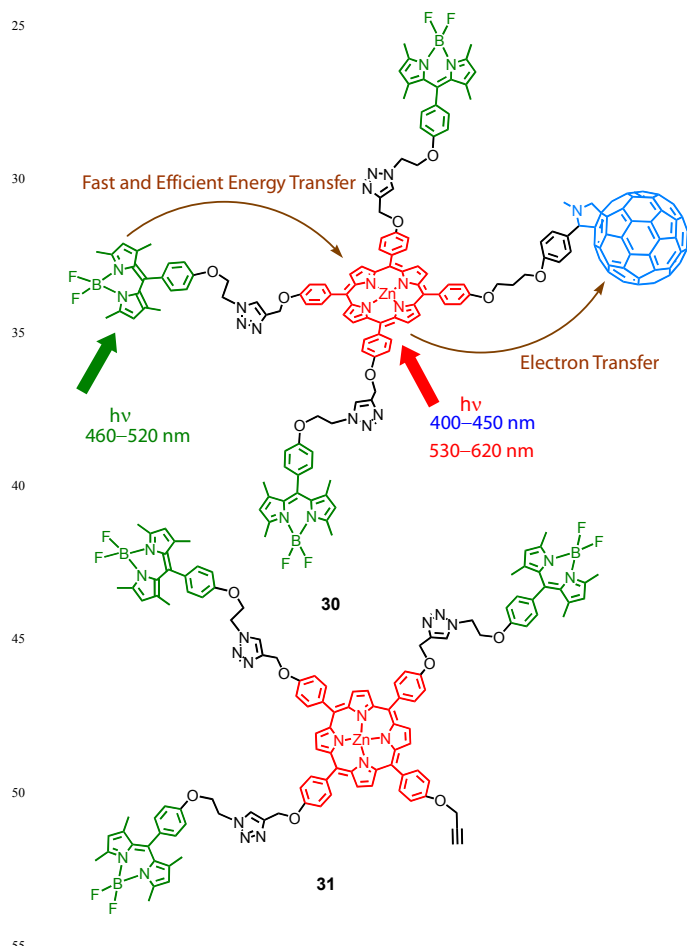


**Fig. 15** Bodipy-porphyrin-C<sub>60</sub> pentad (**30**) with the FRET and PET process (with Zn(II) porphyrin as electron donor and C<sub>60</sub> as the electron acceptor). Compound **31** was used as a reference for study of the photophysical properties.<sup>89</sup>

Femtosecond transient absorption spectra of compound **31** indicates the singlet excited state of the Bodipy moiety was produced upon selective excitation into the Bodipy part (<sup>1</sup>BDP\*). Then the <sup>1</sup>ZnP\* grows in within 400 ps, which was attributed to the FRET with rate constant of  $k = 2.7 \times 10^{10} \text{ s}^{-1}$ . For the pentad **30**, however, the femtosecond transient absorption spectra indicated the production of the singlet excited state of porphyrin was followed by the formation of the radical ion pair (BDP)<sub>3</sub>-ZnP<sup>•+</sup>-C<sub>60</sub><sup>•-</sup>, indicated by the characteristic absorption of the C<sub>60</sub> radical anion at 1000 nm.

Nanosecond transient absorption spectroscopy was used to study the triplet excited state of the compounds. For the reference compound **31**, by excitation either into the ZnP unit (430 nm) or the Bodipy antenna (500 nm), the triplet excited state of ZnP moiety was observed, indicated by the characteristic T<sub>1</sub>→T<sub>n</sub> absorption of <sup>3</sup>ZnP\* at 460 nm and 600–900 nm. The <sup>3</sup>ZnP\* state decay with rate constant of  $1.1 \times 10^4 \text{ s}^{-1}$  (the triplet state lifetime is ca. 90 μs). Thus compound **31** may probably be used as a triplet photosensitizer, showing broadband visible light-absorption.

For the pentad **30**, different nanosecond transient absorption spectra were observed as compared with that of **31**. With photoexcitation into the Bodipy part, the <sup>3</sup>ZnP\* was produced. Decay of the <sup>3</sup>ZnP\* state lead to formation of (BDP)<sub>3</sub>-ZnP<sup>•+</sup>-C<sub>60</sub><sup>•-</sup>. Thus for pentad **30**, singlet and triplet (BDP)<sub>3</sub>-ZnP<sup>•+</sup>-C<sub>60</sub><sup>•-</sup> were produced with the decay of the singlet and triplet excited state of the ZnP part, respectively. The lifetime of the singlet and triplet charge separated state (BDP)<sub>3</sub>-ZnP<sup>•+</sup>-C<sub>60</sub><sup>•-</sup> are 476 ns and 385 ns, respectively. Ground state (S<sub>0</sub> state) was produced by the charge recombination (CR) process. Long-lived charge-separated state is important for research in the area of artificial photosynthesis.<sup>90–95</sup> Ng et al also developed other chromophore conjugates which may be used as broadband visible light-absorbing triplet photosensitizers.<sup>96</sup>

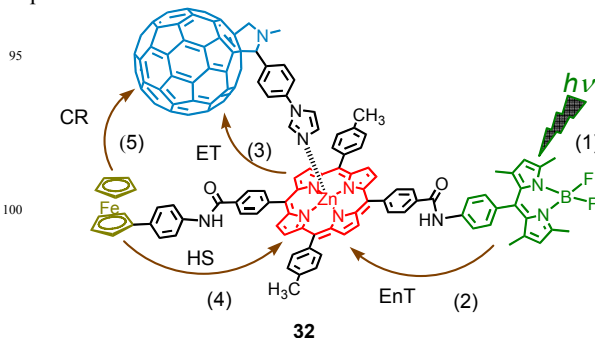


**Fig. 16** Proposed photochemical events in supramolecular Fc-(C<sub>60</sub><sup>•-</sup>Im:ZnP<sup>•+</sup>)-BODIPY (**32**) tetrad featuring a zinc porphyrin (ZnP) as primary electron donor, Bodipy as energy-transferring antenna, ferrocene (Fc) as charge stabilizing HS agent, and fullerene (C<sub>60</sub>Im) as terminal electron acceptor. Abbreviations: EnT = excited energy transfer, ET = excited electron transfer, HS = hole shift, and CR = charge recombination.<sup>97</sup>

Different from the covalent bond profile for attachment of visible light-harvesting Bodipy antenna to the porphyrin chromophore, a novel photosynthetic-antenna–reaction-center model compound, comprised of BF<sub>2</sub>-chelated dipyrromethene (Bodipy) as an energy-harvesting antenna, zinc porphyrin (ZnP) as the primary electron donor, ferrocene (Fc) as a hole-shifting agent, and phenylimidazole-functionalized fulleropyrrolidine

(C<sub>60</sub>Im) as an electron acceptor, has been synthesized and characterized (Fig. 16).<sup>97</sup> Selective photoexcitation of Bodipy resulted in efficient singlet energy transfer to the ZnP moiety. Electron transfer from the <sup>1</sup>ZnP\* or <sup>1</sup>C<sub>60</sub>\* of the coordinated fullerene give the Fc-(C<sub>60</sub>\*Im:ZnP\*)-BODIPY radical ion pair, indicated by the femtosecond transient absorption studies. Subsequent hole migration to the ferrocene entity resulted in the Fc<sup>+</sup>-(C<sub>60</sub>\*Im:ZnP)-BODIPY radical ion pair, for which the lifetime is as long as 7–15 ms.

## 2.5. Supramolecular Bodipy-porphyrin, phthalocyanine or subphthalocyanine conjugates

In a similar way, Guldi et al prepared conjugates with Bodipy antenna axially bound to a Sn(IV) porphyrin via a phenolate or benzoate bridge (Complex **33** and **34**, Fig. 17).<sup>98</sup>

The difference between complexes **33** and **34** is that the bridge between the Sn(IV) and the Bodipy antenna, it is *phenolate* in complex **33**, and it is *benzoate* in complex **34**. The complexes **35** and **36** were used as reference for study of the photophysical properties (Fig. 17). It should be pointed out that although the absorption of Sn(IV) porphyrin coordination center is strong at 425 nm, but the Soret and Q bands at 560 nm and 600 nm are very weak.<sup>98</sup> Thus attaching of Bodipy antenna to the Sn(IV) porphyrin framework is helpful to improve the light-harvesting ability of the complexes in the visible spectral region, and broadband visible light absorption is resulted.<sup>98</sup>

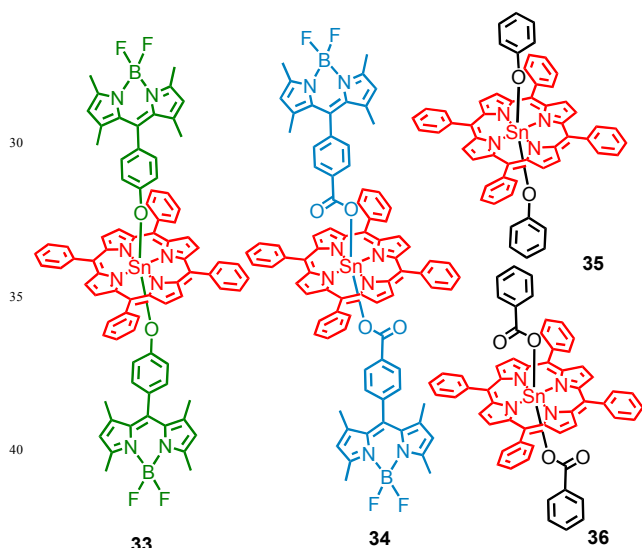


**Fig. 17** The Bodipy-porphyrin conjugates (complexes **33** and **34**) with the Bodipy antenna axially bound to the Sn(IV) centre. Complexes **35** and **36** are reference compounds.<sup>98</sup>

The array **33** shows strong absorption at 425 nm and 500 nm, which are attributed to the Sn(IV) porphyrin coordination moiety and the Bodipy antenna, respectively. The absorption of the array is the sum of the components, thus there is no significant interaction between the chromophores in the array at the ground state. The electrochemical data support this conclusion as well.

The fluorescence emission of the Bodipy antenna was significantly quenched in array **33**, which indicates singlet energy transfer, or electron transfer. The emission of Sn(IV) porphyrin moiety is weak. The reference compound **35**, which is without any Bodipy antenna, also shows much weaker emission as

compared with that of axially OH-coordinated Sn(IV)-porphyrin complex, thus it was concluded that the fluorescence of the Sn(IV) porphyrin moiety was mainly quenched by PET process in complex **33**. For the array **34**, however, upon selective excitation into the Bodipy moiety, the fluorescence emission of the Bodipy antenna was quenched, but the emission of the Sn(IV) porphyrin moiety was not quenched. Thus electron transfer is not significant in array **34**. Moreover, band attributed to the Bodipy moiety was observed in the fluorescence excitation spectra of **34**, thus, no significant PET exists in array **34**, and the quenching is due to singlet energy transfer from the Bodipy antenna to the Sn(IV) porphyrin moiety.<sup>98</sup>

Femtosecond transient absorption spectra of the complexes were studied. For array **34**, upon selective excitation into the Bodipy antenna, the singlet state of the antenna decay with much faster kinetics  $3.5 \pm 1$  ps, as compared with the Bodipy reference, for which the decay time of the singlet excited state is  $3.5 \pm 0.5$  ns. The product of the decay is the singlet excited state of the Sn(IV) porphyrin moiety, indicated by the minima at 435, 560, 600, and 660 nm as well as a broad maximum between 445 and 600 nm. Then the singlet excited state of the Sn(IV) porphyrin undergoes the ISC to produce triplet excited state.<sup>98</sup>

For the array **33**, however, the photophysical processes are different. Upon selective excitation into Bodipy antenna in array **33**, firstly the singlet excited state of the Bodipy antenna was produced. Then the singlet excited state of the porphyrin moiety was produced by a fast energy transfer ( $2.0 \pm 0.5$  ps). Then a charge transfer state (CTS) was formed with a kinetic of  $4 \pm 2$  ps, indicated by the absorption at 460, 485, 545, 585, 615, and 645 nm, which resemble the one-electron-reduced porphyrin anion. The charge recombination (CR) takes ca.  $450 \pm 50$  ps.

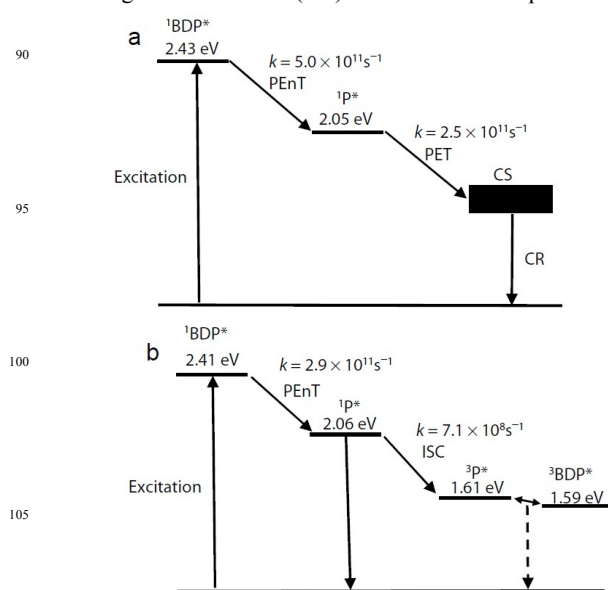


**Fig. 18** Jablonski diagrams illustrating the processes that take place after photoexcitation of the Bodipy part of (a) **33** and (b) **34**. Rate constants,  $k$ , of the processes as measured by transient absorption spectroscopy are also shown. <sup>1</sup>BDP\* and <sup>1</sup>p\* denote the Bodipy and porphyrin-based singlet excited states, respectively, while <sup>3</sup>BDP\* and <sup>3</sup>p\* denote the corresponding triplets. PET stands for photoinduced electron transfer, PEnT for photo-induced energy transfer, and ISC for intersystem crossing. Dashed arrow denotes radiationless decay. Reproduced with permission from Lazarides et al.<sup>98</sup>

The energy transfer mechanism was proposed to be via the Förster mechanism, based on the match of the calculated Förster energy transfer rate constant and the experimental results. However, the triplet state property of the arrays were not studied in detail, for which the nanosecond transient absorption spectroscopy is required. Moreover, the arrays were not studied for any applications. But we envision that the complexes are interesting for applications in photocatalytic hydrogen ( $H_2$ ) production, or other photocatalysis. The photophysical processes involved in arrays **33** and **34** can be summarized in Fig. 18.

Similar approach was also used for preparation of Bodipy-subphthalocyanine arrays, with the Bodipy antenna axially bound to the B atom of SubPc (Fig. 19).<sup>99</sup> The subPc unit gives strong absorption at 563 nm ( $\log \epsilon = 4.96$ ), and the Bodipy unit gives absorption at 502 nm ( $\log \epsilon = 5.06$ ). The styrylBodipy in **38** gives absorption at 562 nm ( $\log \epsilon = 5.02$ ). Thus singlet energy transfer from the Bodipy to the SubPc unit was observed in array **37**, whereas in array **38** the singlet energy transfer is from subPc to the styrylBodipy moiety. The energy transfer process was not studied with femtosecond transient absorption. Although the triplet excited state was not studied, formation of triplet excited state, especially in array **37**, is expected since it is known that subPc undertakes efficient ISC (triplet state quantum yield is up to  $\Phi_T = 70\%$ ).<sup>100,101</sup> For dyad **38**, however, the ISC may be in competition with the FRET to the styrylBodipy unit.<sup>102,103</sup>

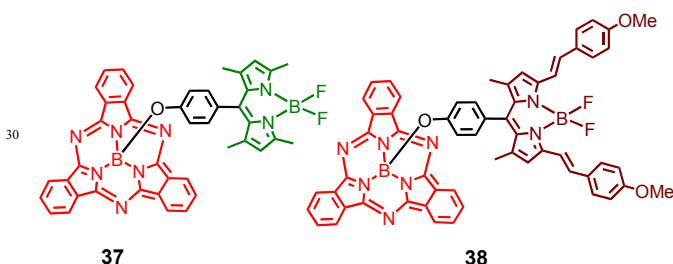


**Fig. 19** Broadband visible light-absorbing Bodipy-subphthalocyanine conjugates **37** and **38**.<sup>99</sup>

Similarly BODIPY-phthalocyanine conjugates were prepared, with the Bodipy antenna axially bound to the Si atom (Fig. 20).<sup>104,105</sup> In these triads, the Bodipy antenna show strong absorption at 502 nm ( $\log \epsilon = 5.31$ ), whereas the phthalocyanine gives strong absorption at 683 nm ( $\log \epsilon = 5.44$ ). The styrylBodipy units in triad **40** gives absorption at 571 nm ( $\log \epsilon = 5.40$ ). For triad **39**, the singlet energy transfer from the Bodipy unit to the phthalocyanine unit is predominant, whereas for triad **40**, the electron transfer is significant. Phthalocyanine part (energy acceptor) in triad **39** gives fluorescence quantum yield of 60%, whereas in triad **40** the phthalocyanine part gives fluorescence quantum yield of only 0.3%.

The triplet excited state of the triads were not studied. Study of the triplet state property of triad **39** will be interesting, since it was reported that phthalocyanine derivatives show efficient ISC.<sup>106–108</sup> Besides the energy transfer, phthalocyanine was also used for construction of molecular arrays for photoinduced charge transfer.<sup>109</sup>

The molecular arrays discussed in the above sections show broadband visible light absorption. However, it should be pointed out that most of the above chromophore conjugates were not designed as triplet photosensitizer. In most of the cases, the triplet

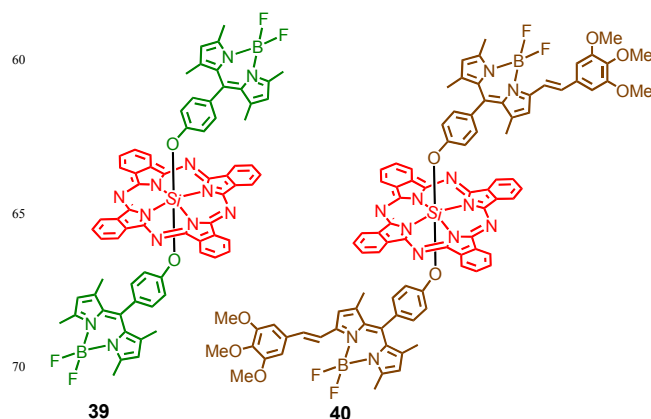


**Fig. 20** Broadband visible light-absorbing subphthalocyanine triads **39** and **40**.<sup>104,105</sup>

states were not studied in detail with the nanosecond transient absorption spectroscopy. Based on the widely used FRET approach for attaining broadband visible light absorption in the areas of fluorescent molecule sensors,<sup>110,111</sup> we designed organic chromophore conjugates to attain broadband visible light absorption. Moreover, the singlet energy acceptors in these chromophore conjugates play the role of spin converter, i.e. for triplet state formation.

## 2.6. Broadband visible light-absorbing chromophore conjugates as triplet photosensitizers

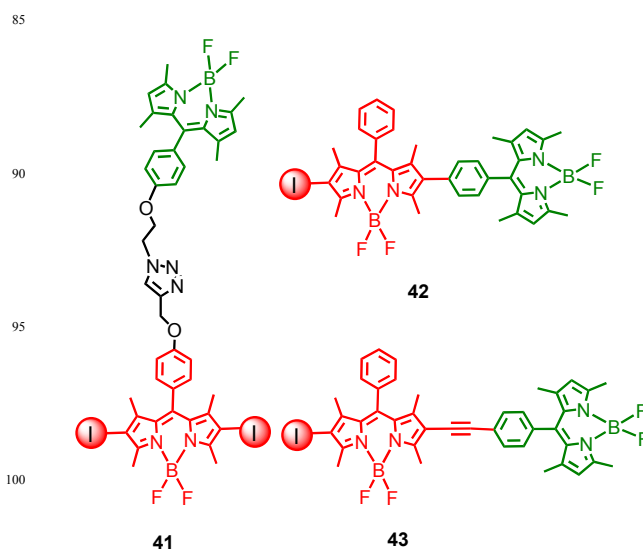


**Fig. 21** Bodipy-diiodoBodipy dyads as triplet photosensitizers (**41**, **42**, **43**) (Bodipy moiety is the energy donor, iodoBodipy moiety is the energy acceptor and the spin converter).<sup>56</sup>

We designed the dyads with Bodipy and iodoBodipy moieties (Fig. 21).<sup>56</sup> In **41**, **42** and **43**, Bodipy moiety gives shorter absorption wavelength, and its emission band overlaps with the absorption of the diiodoBodipy moiety. FRET is ensured for this dyad and the similar dyads **42** and **43**. Moreover, the diiodoBodipy moiety in **41** is the spin converter, since efficient ISC was observed for the diiodoBodipy moiety previously.<sup>112–115</sup> The absorption wavelength range of **41**, **42** and **43** is broader than the diiodoBodipy (**12**) (Fig. 22a).

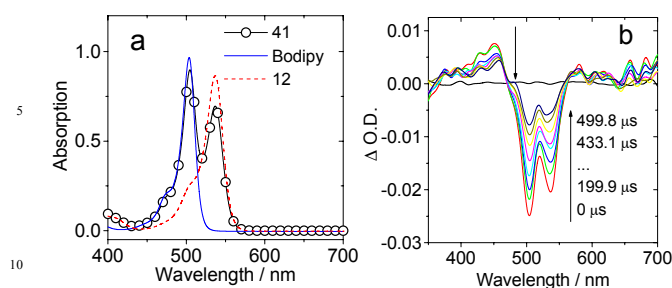


**Fig. 22** (a) The UV-vis absorption of **41** and the energy donor and energy acceptor reference compounds (**12** and Bodipy), in toluene,  $c = 1.0 \times 10^{-5}$  M. (b) The nanosecond transient absorption of **41** in deaerated toluene,  $\lambda_{\text{ex}} = 532$  nm,  $c = 1.0 \times 10^{-6}$  M,  $20^\circ\text{C}$ .<sup>56</sup>

In order to study the triplet excited states of the dyad triplet photosensitizers, the nanosecond transient absorption spectra of **41**, **42** and **43** were studied (exemplified with **41** in Fig. 22b). Interestingly, we found that the triplet excited state of **41** is delocalized on the Bodipy and the diiodoBodipy moieties of **41**, indicated by the two bleaching band at 504 nm and 536 nm, respectively.<sup>56</sup> The Bodipy and the diiodoBodipy moieties give steady state absorption at these wavelengths, respectively. Since there is no  $\pi$ -conjugation between the two chromophores, and the two bleaching bands decay with the same kinetics, a triplet state equilibrium was proposed for **41**. Time-dependent DFT (TDDFT) computations indicated that the  $T_1$  and  $T_2$  states of **41**, which is confined on the two chromophores, respectively, are degenerated (with same energy levels). Herein forward singlet energy transfer from the Bodipy moiety to the iodoBodipy moiety occurs, and followed by the backward triplet energy transfer from the diiodoBodipy to the Bodipy moiety, i. e. the ping-pong energy transfer and triplet state equilibrium was established. To the best of our knowledge, this is the first time that such photophysical processes were observed for an organic molecular conjugate.<sup>65,116</sup>

It should be pointed out that the intramolecular triplet state energy transfer in **41** is fast ( $k > 10^8$  s<sup>-1</sup>). We also studied the intermolecular triplet energy transfer between the iodoBodipy and Bodipy. The results show that the intermolecular TTET is much slower (Fig. 23). Moreover, no triplet state equilibrium was observed, and the TTET is uni-directional.

The dyad triplet photosensitizers **41**, **42** and **43** were used for photosensitizing singlet oxygen ( $^1\text{O}_2$ ), with broadband photoexcitation (white light from a xenon arc lamp). The results show that the  $^1\text{O}_2$  photosensitizing of the dyad triplet photosensitizers are more efficient than the diiodoBodipy.<sup>56</sup> These results show that broadband visible light-absorbing triplet photosensitizers are more efficient than the mono-chromophore based triplet photosensitizers.

In order to obtain broader visible light-absorption band, and to explore more diverse molecular structure for the triplet photosensitizers based on FRET effect, we used Bodipy, or carbazole-conjugated Bodipy as energy donor (for variable absorption wavelength), and diiodo-azaBodipy at the energy acceptor and the spin converter to prepare triplet photosensitizers, thus triad **44** and **45** were prepared, with **46** as the reference compound (Fig. 24).<sup>58</sup>

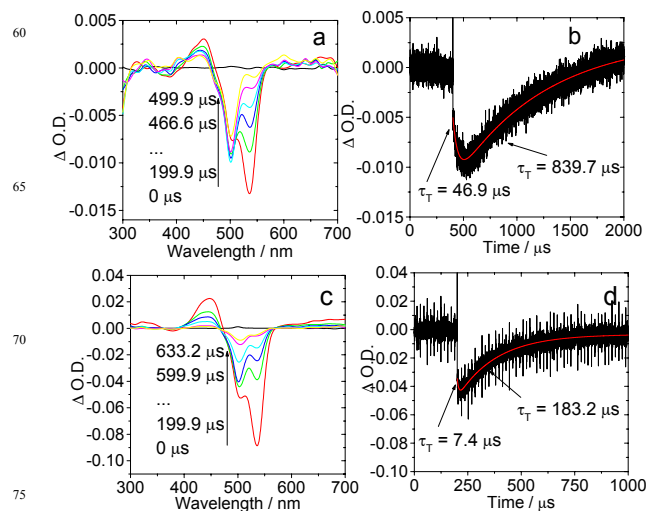


**Fig. 23** Intermolecular triplet-triplet-energy-transfer (TTET) observed with nanosecond transient absorption spectra. (a)  $c[\text{Bodipy}] = 5.0 \times 10^{-6}$  mol/L,  $c[\text{Bodipy}] : c[\text{12}] = 5:1$ , (b) The decay trace at 500 nm, (c)  $c[\text{Bodipy}] = 1.0 \times 10^{-5}$  mol/L,  $c[\text{Bodipy}] : c[\text{12}] = 1:1$ . (d) The decay trace at 500 nm,  $\lambda_{\text{ex}} = 535$  nm. In Toluene.  $20^\circ\text{C}$ .

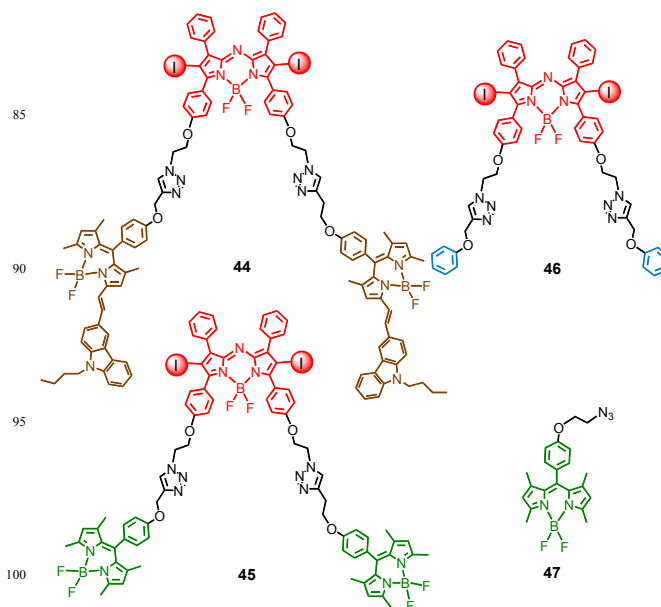


**Fig. 24** Diiodo-azaBodipy derived broadband visible light-absorbing triplet photosensitizers **44**, **45**, **46** and **47**.<sup>58</sup>

Diiodo-azaBodipy gives absorption at 683 nm, the Bodipy moiety or the carbazole-conjugated Bodipy moiety give absorption at 503 nm and 594 nm, respectively. Thus two absorption bands were observed for **44** and **45**, whereas for **46**, only one absorption band was observed (Fig. 25). With fluorescence quenching study and comparison of the fluorescence excitation spectra with the UV-vis spectra (Fig. 25b), we confirmed the singlet energy transfer in **44** and **45**. It should be pointed out that the singlet energy transfer mechanism for **45** may be through-bond-energy-transfer (TBET), not FRET, because the spectral overlap integral is small.

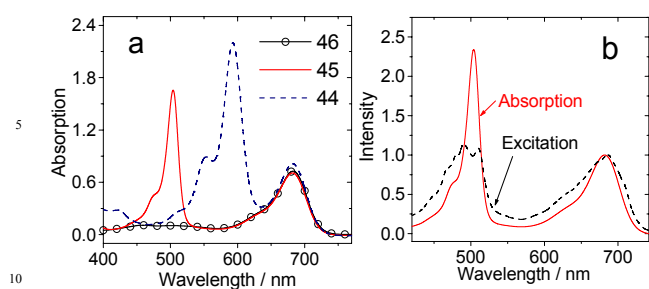


**Fig. 25** (a) UV-vis absorption spectra of **44**, **45** and **46**. (b) Comparison of the fluorescence excitation spectrum with the UV-vis absorption spectrum of **45** ( $\lambda_{em} = 760$  nm). ( $c = 1.0 \times 10^{-5}$  M in toluene, 20 °C).<sup>58</sup>

It should be pointed out that the singlet energy transfer such as FRET was usually evaluated by the quenching of the fluorescence of the energy donor. However, this is not a reliable method because photophysical processes other than the FRET can also quench the fluorescence of the energy donor, such as photo-induced electron transfer (PET). This scenario was demonstrated by the quenching of the fluorescence of the energy donor in **45** (Fig. 26). It is obvious that the fluorescence of the energy donor was almost completely quenched. Quantitative EnT will be postulated based on the quenching study. Calculation of the Gibbs free energy transfer of **45** indicated that PET is also possible for the quenching of the energy donor's fluorescence.

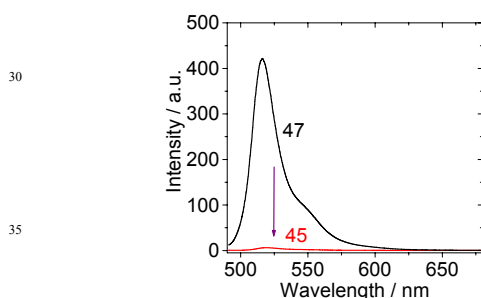


**Fig. 26** Fluorescence emission spectra of **47** and the triplet photosensitizer **45**,  $\lambda_{ex} = 490$  nm.  $c = 1.0 \times 10^{-5}$  M in toluene 20 °C.<sup>58</sup>

In order to study the triplet excited state property of the Bodipy-azaBodipy triads, the nanosecond transient absorption spectra of the triads were studied (Fig. 27). Upon nanosecond pulsed laser excitation at 355 nm (both Bodipy and iodo-AzaBodipy are photoexcited), bleaching band at 668 nm was observed. Interestingly, no bleaching band at 503 nm was observed. These results indicate that the  $T_1$  excited state of **45** is exclusively confined on the diiodoAzaBodipy moiety, and the Bodipy moiety makes no contribution to the  $T_1$  state of **45**. This result is due to the lower  $T_1$  state energy level of the azaBodipy (1.22 eV),<sup>117</sup> as compared with that of the Bodipy moiety (1.69 eV).<sup>78,118,119</sup> Similar results were observed for **44**.<sup>58</sup>

The singlet energy transfer process in **45** was studied with the femtosecond transient absorption spectra (Fig. 28). Upon femtosecond pulsed laser excitation at 504 nm, where the absorption is dominated by the Bodipy moiety (energy donor), the bleaching band at 505 nm decreased, at the same time, the bleaching band at 680 nm grows. This process indicates the singlet

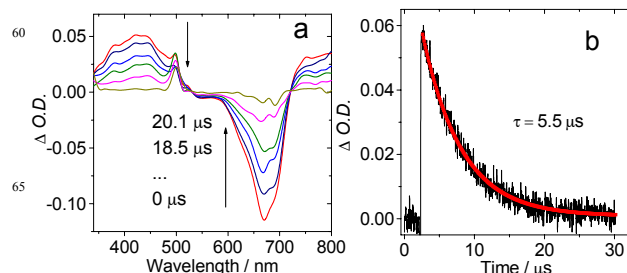


**Fig. 27** (a) Nanosecond transient absorption spectra of **45**. (b) The decay of **70** was monitored at 430 nm. After pulsed excitation at 355 nm ( $c = 2.0 \times 10^{-5}$  M, in deaerated toluene, 20 °C).<sup>58</sup>

energy transfer in **45**. The energy transfer rate constant is  $k_{EnT} = (4.3 \pm 0.3) \times 10^{10} \text{ s}^{-1}$ . In comparison, the singlet energy transfer of **44** is with a fast kinetics,  $k_{EnT} = (5.1 \pm 0.4) \times 10^{11} \text{ s}^{-1}$ . The faster singlet energy transfer in **44** is attributed to the larger spectral overlap integral for **44**. We confirmed that the broadband visible light-absorbing **44** and **45** is more efficient than **46** in  $^1\text{O}_2$  photosensitizing.

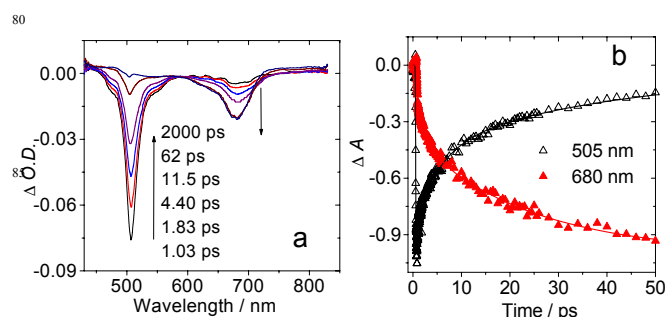


**Fig. 28** (a) Femtosecond transient absorption spectra of dyad **45** upon pulsed laser excitation ( $\lambda_{ex} = 504$  nm) in toluene; (b) Decay trace at 505 and 680 nm. 20 °C.<sup>58</sup>

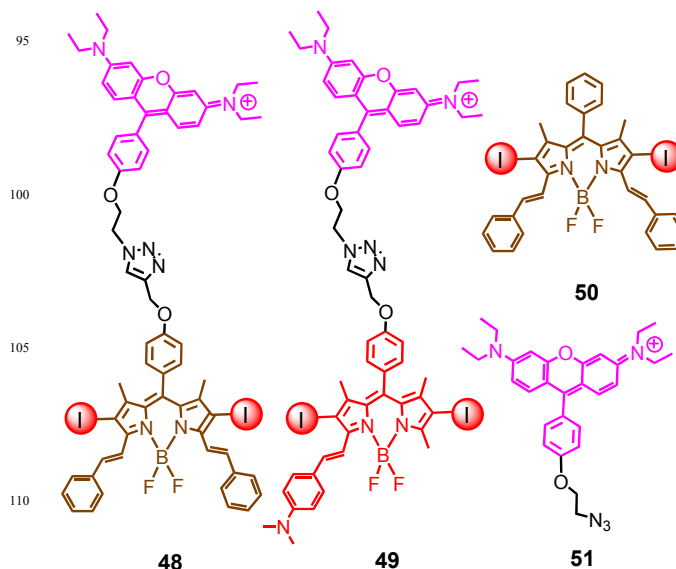


**Fig. 29** Rhodamine-diiodo-styrylBodipy dyad triplet photosensitizers (**48**, **49**, **50** and **51**) which give broadband visible light-absorption.<sup>57</sup>

Rhodamine is a well known visible light-absorbing chromophore, and has been widely used in preparation of FRET molecular dyads, mainly concerning singlet excited state manifold, i.e. fluorescence, such as visible light-harvesting molecular assemblies and molecular probes. However, no application of rhodamine in construction of organic triplet photosensitizer was reported.

On the other hand, rhodamine derivatives usually contain carboxylic moiety, which may complicate the photophysical property due to the reversible spiroactam $\leftrightarrow$ opened amide transformation.<sup>120</sup> The spiroactam form gives no visible light-absorption and the opened amide form give strong absorption at ca. 570 nm. In order to eliminated this complicity, we used rhodamine moiety which is without the carboxylic moiety for construction of broadband visible light absorbing triplet photosensitizers **48** and **49** (Fig. 29).<sup>57</sup>

In **48** and **49**, rhodamine was used as energy donor and diiodostyrylBodipy was used as energy acceptor, as well as spin converter. The UV-vis absorption of **48** (Fig. 30) indicated that there is no strong interaction between the components at ground state. Fluorescence quenching of the rhodamine part in **48**, and the comparison of the fluorescenc excitation spectrum and the UV-vis absorption spectrum of **48** supports the singlet energy transfer process.

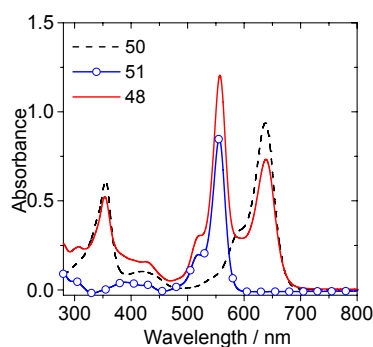


**Fig. 30** UV-vis absorption of **48**, **50** and **51**.  $c = 1.0 \times 10^{-5}$  M, in  $\text{CH}_2\text{Cl}_2$ , 20 °C. Reproduced with permission from Ma et al.<sup>57</sup>

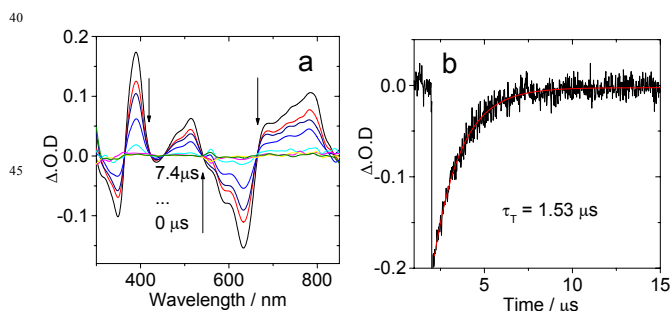


**Fig. 31** (a) Nanosecond transient absorption spectra of **48** ( $\lambda_{\text{ex}} = 532$  nm). (b) Decay curve of **48** at 630 nm,  $c = 1.0 \times 10^{-5}$  M, in deaerated  $\text{CH}_2\text{Cl}_2$ , 20 °C.<sup>57</sup>

The nanosecond transient absorption spectroscopy shows that the  $T_1$  state of **48** is confined on the diiodostyrylBodipy moiety (Fig. 31). The triplet state lifetime is 1.53  $\mu\text{s}$  (Fig. 31b). Note the uniodinated styrylBodipy shows much longer triplet excited state lifetime, for example in styrylBodipy- $\text{C}_{60}$  dyad (71.5  $\mu\text{s}$ ). The

triplet formation with **49** is weak in polar solvents, such as acetonitrile. This effect may be attributed to the quenching of the triplet state by intramolecular charge transfer (ICT) in the styrylBodipy part in **49**.<sup>57</sup>

The dyad triplet photosensitizers were used for photoredox catalytic organic reactions (Fig. 32), i.e. oxidation/[3 + 2] cycloaddition/aromatization tandem reaction with tetrahydroisoquinoline derivatives.<sup>51,57</sup>

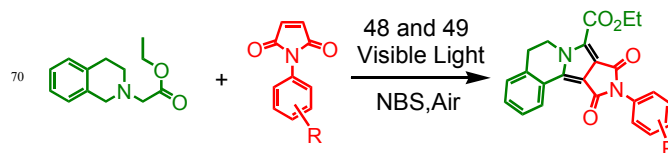


**Fig. 32** Oxidation/[3 + 2] cycloaddition/aromatization tandem reaction with tetrahydroisoquinoline derivatives catalyzed by organic triplet photosensitizers **48** and **50**.<sup>57</sup>

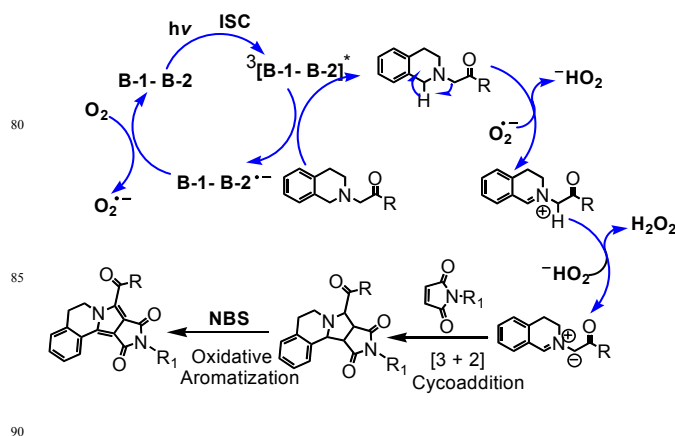


**Fig. 33** Photocatalytic oxidation-cycloaddition-aromatization sequence with the organic triplet photosensitizers **48** and **50**. Reproduced with permission from Ma et al.<sup>57</sup>

The reaction mechanism were studied with electron spin resonance (ESR) spectroscopy. It was supposed that the triplet excited state of **48** acts as electron acceptor, the isotetrahydroquinoline is the electron donor (Fig. 33). Upon photoexcitation of the **48**, and the following intermolecular electron transfer, iminium was formed. 5,5-dimethyl-1-pyrroline-*N*-oxide (DMPO) and 2,2,6,6-tetramethylpiperidine (TEMP) were employed as scavengers for  $\text{O}_2^{\cdot-}$  and  $^1\text{O}_2$ , respectively. Therefore the electron transfer from the amine substrate to the organic triplet photosensitizer is confirmed, i.e. the photocatalytic reaction proceeds with  $\text{O}_2^{\cdot-}$  as one of the crucial species, not  $^1\text{O}_2$  (Fig. 33). Upon white light photoexcitation (broadband light source), the photocatalytic efficiency of **R-1** is higher than that of **B-1**, which demonstrated that the broadband visible light-absorbing triplet photosensitizer is superior to the mono-visible light-harvesting chromophore triplet photosensitizers. It should be pointed out application of the efficient new triplet photosensitizers as photocatalysts in photoredox catalytic organic reactions is still in the very early age. We envisage that more application of the new triplet photosensitizers in photocatalysis will be witnessed.

Recently a polymeric broadband visible light-absorbing triplet

photosensitizer was designed (Fig. 34).<sup>121</sup> In the polymer backbone, the fluorene and Bodipy units were copolymerized as the singlet energy donor, as well as the UV-green light-harvesting units. Diiodo-StyrylBodipy units were dangled on the fluorene unit, as the singlet energy acceptor and the spin converter. As a result the polymer shows broadband absorption in the range of 400–700 nm. It was confirmed the polymeric triplet photosensitizer is more efficient than the diiodostyrylBodipy alone for photosensitizing of  $^1\text{O}_2$ .

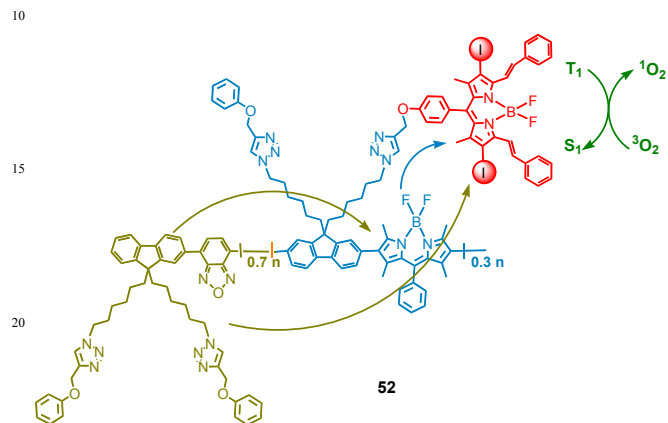


**Fig. 34** Polymeric broadband visible light-absorbing triplet photosensitizer (**52**). Reproduced with permission from He et al.<sup>121</sup>

### 2.7. $\text{C}_{60}$ as the Spin converter in broadband visible light-absorbing heavy atom-free triplet photosensitizers

Up to now most of the triplet photosensitizers are dependent on heavy atom effect, with which the ISC is facilitated. The same hold for the broadband absorbing triplet photosensitizers such as **52**, in which the spin converter is diiodoBodipy derivatives. Previously it was reported that for oligothiophene and azaBodipy antenna dyads with  $\text{C}_{60}$ , population of triplet excited state was observed upon photoexcitation (Fig. 35).<sup>122,123</sup> In some cases it was attributed to the CR process. However, it is well known that  $\text{C}_{60}$  shows efficient ISC (close to unity),<sup>124</sup> thus a cascade singlet energy transfer and ISC of the  $\text{C}_{60}$  moiety may play the role for triplet production with these dyads.

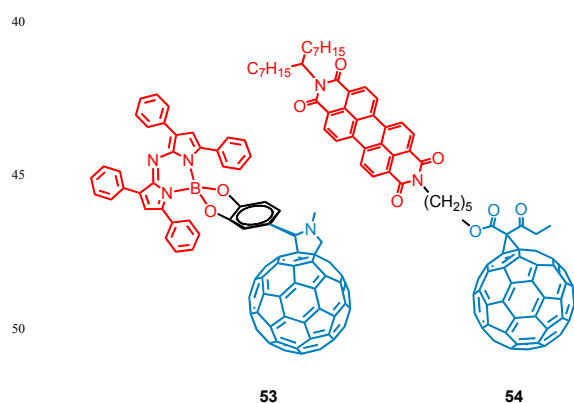


**Fig. 35** AzaBodipy- $\text{C}_{60}$  (**53**)<sup>122</sup> and PBI- $\text{C}_{60}$  dyads (**54**)<sup>123</sup> with triplet excited state populated upon photoexcitation.

Recently we proposed to use the ISC capability of fullerene  $\text{C}_{60}$  for preparation of heavy atom free triplet photosensitizers

(Fig. 36).<sup>46,125,126</sup> These heavy-atom-free triplet photosensitizers were used for TTA upconversion,<sup>46</sup> and photoredox catalytic organic reactions,<sup>48,58</sup> and the efficiency of these organic heavy atom-free triplet photosensitizers is satisfactory. High  $^1\text{O}_2$  quantum yields ( $\Phi_{\Delta} = 0.85$ ) and TTA upconversion quantum yield were observed. Using of a  $\text{C}_{60}$  unit as the spin converter is better than using a spin converter which is dependent on the heavy atom effect, because ISC may *not* be facilitated by heavy atoms if the intrinsic decay of the  $\text{S}_1$  state of the chromophore is ultrafast.<sup>67</sup> In other words, attaching heavy atoms to chromophore does not always guarantee efficient ISC.

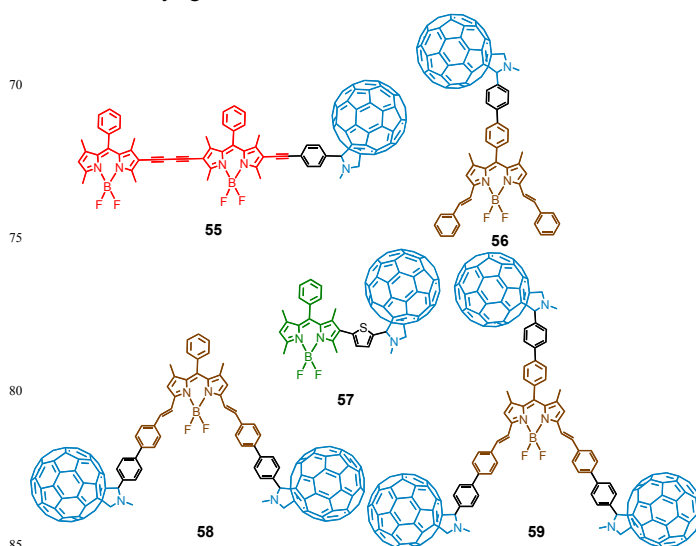


**Fig. 36** Representative  $\text{C}_{60}$ -Bodipy heavy atom-free triplet photosensitizers (**55**, **56**, **57**, **58**, **59**).<sup>46,125,126</sup>

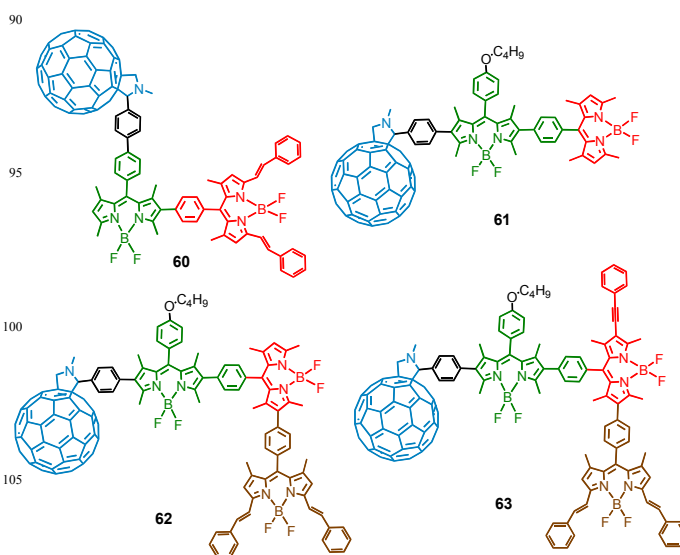


**Fig. 37** Representative broadband visible light-absorbing  $\text{C}_{60}$ -Bodipy heavy atom-free triplet photosensitizers (**60**, **61**, **62**, **63**).<sup>48</sup>

In order to attain broadband visible light absorption, we used  $\text{C}_{60}$  as spin converter and more than one Bodipy unit as light-harvesting antenna for preparation of heavy atom-free broadband

visible light-absorbing triplet photosensitizers (Fig. 37).<sup>8,48</sup> The strategy is to attach different antenna to C<sub>60</sub> to attain broadband absorption visible light, and the harvested photoexcitation energy can be funneled to the C<sub>60</sub> moiety. The ISC of C<sub>60</sub> moiety will convert the photoexcitation energy to triplet state. We selected Bodipy as the principle chromophore due to the feasible derivatization.<sup>48</sup>

In compound **60**, the two Bodipy moieties are with different conjugation frameworks, thus the absorption wavelength of the two Bodipy moieties are at 517 nm and 629 nm, respectively. Note the S<sub>1</sub> state energy level of C<sub>60</sub> is 1.75 eV, thus singlet energy transfer from the two Bodipy moieties to C<sub>60</sub> is possible. At least with the antenna alone, we confirmed the FRET effect, although the detail photophysics of **60** were not studied with femtosecond transient absorption spectroscopy.

The triplet excited state of the triad was studied with nanosecond transient absorption spectra (Fig. 38), upon selectively excitation into the Bodipy antenna, the triplet excited state is confined on the styrylBodipy moiety, neither on the C<sub>60</sub> moiety or Bodipy moiety.<sup>48</sup> This result can be rationalized by the different triplet state energy levels of the three moieties. These results indicate that ping-pong energy transfer occurred for **60**, i.e. the forward singlet energy transfer from the Bodipy moieties to the C<sub>60</sub> moiety, and the backward fast triplet energy transfer from the C<sub>60</sub> moiety to the styrylBodipy moiety (rate constants > 10<sup>8</sup> s<sup>-1</sup>).

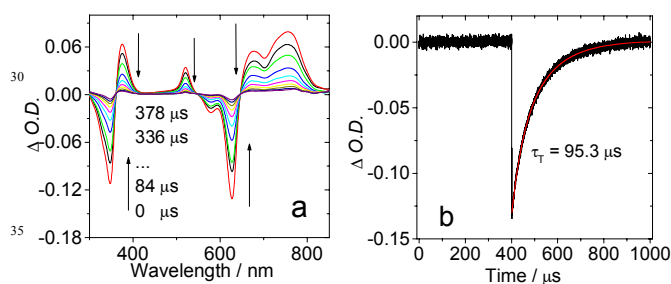


**Fig. 38** Nanosecond transient absorption spectra of **60**. (a) Transient absorption spectra and (b) the decay trace of the ground state bleaching at 630 nm.<sup>48</sup>

We found that the Bodipy-C<sub>60</sub> broadband visible light-absorbing triplet photosensitizers are efficient <sup>1</sup>O<sub>2</sub> photosensitizers (with Φ<sub>Δ</sub> up to 81–92%).<sup>48</sup> Moreover, the compounds were used as electron donor to produce superoxide radical anion (O<sub>2</sub><sup>•-</sup>) in the presence of sacrificial electron donor such as *N,N*-diisopropylethylamine. Thus these compounds were used as photocatalyst for photocatalytic aerobic oxidation of aromatic boronic acids to produce phenols. The reaction times are much shorter as compared with that of the conventional photocatalyst such as Eosin Y (**3**). Thus the Bodipy-C<sub>60</sub> triads can be used as dual functional photocatalysts, either as <sup>1</sup>O<sub>2</sub> photosensitizer, or as electron donor to produce superoxide radical anion (O<sub>2</sub><sup>•-</sup>) for aerobic oxidation of aromatic boronic acids to produce phenols.

## 2.8. Pt(II) complexes show broadband visible light absorption

Previously broadband visible light-harvesting transition metal complexes were reported.<sup>65,86,127</sup> However, much room is left for

preparation of Pt(II) complexes with feasibly derivatizable molecular structures. Concerning this aspect, the trans bis(trialkylphosphine) Pt(II) bisacetylide complexes are in particular interest, because different alkynyl ligands can be induced by a stepwise approach.<sup>127–130</sup> Thus we envisaged to prepare trans bis(phosphine) Pt(II) bisacetylide complexes which show broadband visible light absorption (Fig. 39).<sup>64</sup>

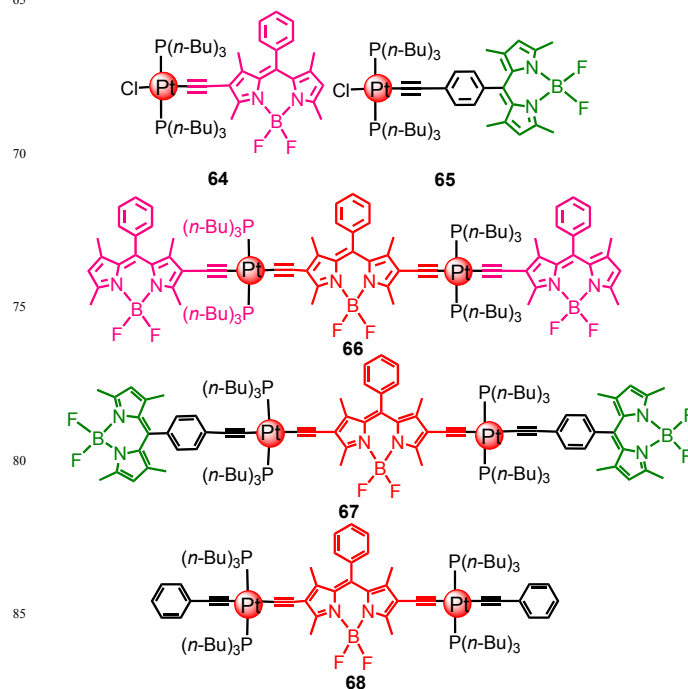


**Fig. 39** The broadband visible light-absorbing trans bis(tri-*n*-butylphosphine) complexes **66** and **67**. The complexes **64**, **65** and **68** containing a mono visible light-absorbing ligand were used as reference complexes.<sup>64</sup>

The design rationals for complexes **66** and **67** is that the bimetalated 2,6-diethynylBodipy will show red-shifted absorption as compared with that of the mono-metalated 2-ethynylBodipy ligand.<sup>131</sup> Thus **66** will show broad band visible light absorption. Moreover, it is expected that the ISC of the central coordinated Bodipy ligand is efficient,<sup>8</sup> therefore the broadband visible light photoexcitation energy harvested by **66** can be efficiently funneled to the triplet state manifold. The lowest-lying triplet excited state (T<sub>1</sub> state) of **66** is confined on the central coordinated Bodipy ligand. The same design rational was applied for **67**. In **67**, however, the peripheral coordinated Bodipy ligand will show absorption at ca. 500 nm because the coordinated center is not attached to the π-core of the Bodipy.<sup>131</sup> Thus more distinct absorption bands will be observed for **67** as compared to that of **66**.

The UV–vis absorption spectra of the complex show that **66** shows broadband absorption in the range of 500–700 nm, whereas **67** shows absorption bands in the range of 450–700 nm, and the two absorption bands of **67** are almost baseline-separated (Fig. 40). For **66**, the two absorption bands are almost merged. Quenching of the energy donor and the comparison of the luminescence excitation and UV–vis absorption spectra indicated the singlet energy transfer process in **66** and **67**.<sup>80</sup>

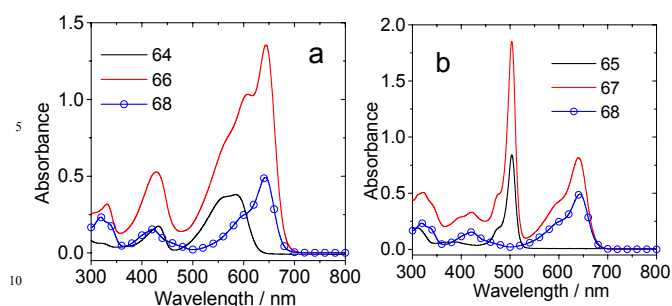


**Fig. 40** UV-vis absorption spectra of the complexes. (a) Complexes **64**, **66** and **68**. (b) Complexes **65**, **67** and **68**.  $c = 1.0 \times 10^{-5}$  M in toluene at 20 °C.<sup>64</sup>

The FRET process was confirmed by the femtosecond transient absorption spectroscopy (Fig. 41). Upon selective excitation into the energy donor, two bleaching bands were observed at 505 nm and 650 nm. Along with the decrease of the bleaching band at 505 nm, the bleaching band at 650 nm grows. These processes indicated the FRET process in **67**. The rate constants of the singlet energy transfer process was calculated as  $k_{\text{EnT}} = 4.0 \times 10^{10} \text{ s}^{-1}$ .

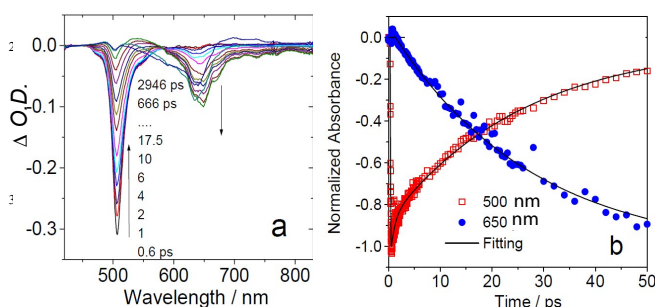


**Fig. 41** Picosecond ultrafast transient absorption spectra of **67** upon femtosecond pulsed laser excitation at 504 nm. (a) Transient absorption spectra after pulsed laser excitation at 504 nm. (b) Decay traces at 500 nm and 650 nm.  $c = 1.0 \times 10^{-5}$  M in toluene at 20 °C.<sup>64</sup>

The FRET process was confirmed by the femtosecond transient absorption spectroscopy (Fig. 41). Upon selectively excitation into the energy donor, two bleaching bands were observed at 505 nm and 650 nm. Along with the decrease of the bleaching band at 505 nm, the bleaching band at 650 nm grows. These processes indicated the FRET process in **67**. The rate constants of the singlet energy transfer process was calculated as  $k_{\text{EnT}} = 4.0 \times 10^{10} \text{ s}^{-1}$ .

In order to study the triplet excited state of the triads **66** and **67**, nanosecond transient absorption spectra were studied.<sup>64</sup> The results show that the  $T_1$  states of **66** and **67** are confined on the central coordinated Bodipy ligands. The  $T_1$  state energy level of the centrally coordinated Bodipy ligand can be approximated as 1.50 eV by the phosphorescence emission, which is lower than the peripheral Bodipy ligands, for which the  $T_1$  state energy level is 1.69 eV. The results of the nanosecond transient absorption spectroscopy indicated that the ISC rate constant of **67** is at least  $1 \times 10^8 \text{ s}^{-1}$ , and that there is no triplet state equilibrium.<sup>56</sup>

The advantage of using trans bis(tributylphosphine) Pt(II) bisacetylide complexes is that different light-harvesting ligands

can be easily introduced to the complex. Different ligands pairing may exert significant impact on the intramolecular energy transfer or electron transfer process, and the property of the triplet excited state may vary substantially. Following this line, we prepared a Bodipy-NDI dyad (**69**, Fig. 42). Complexes **70** and **71**, which contain only one visible light-harvesting chromophore, were used as reference complexes in the studies.<sup>132</sup>

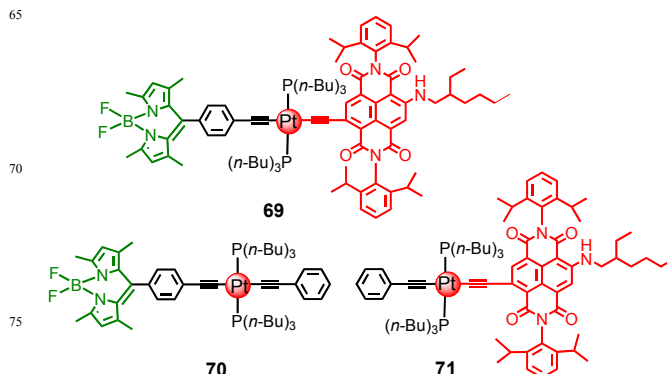


**Fig. 42** Broadband visible light-absorbing trans bis(tributylphosphine) Pt(II) bis(acetylide) complex **69** and the reference complexes which contain only a single visible light-harvesting ligand.<sup>132</sup>

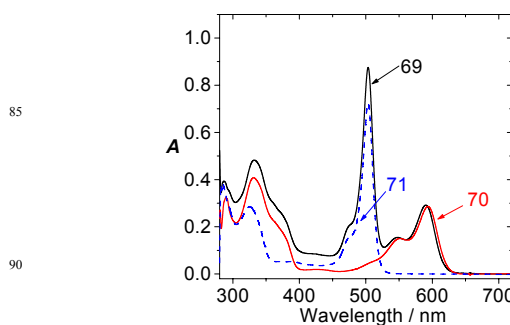


**Fig. 43** UV-vis absorption of Pt(II) complexes.  $c = 1.0 \times 10^{-5}$  M, in toluene at 20 °C.<sup>132</sup>

The UV-vis absorption spectrum of **69** is the sum of that of **70** and **71** (Fig. 43). Thus there is no  $\pi$ -conjugation between the NDI and the Bodipy chromophores in **71** across the Pt(II) coordination center. In other words, the Franck-Condon state is *localized* on the respective chromophores. Previously it was proposed that the Franck-Condon state may be *de-localized*. Application of heteroleptic ligands giving drastically different absorption in the complexes is helpful for elucidate the issue.

Comparison of the luminescence excitation spectra with the UV-vis absorption spectra indicates the singlet energy transfer from the Bodipy unit to the NDI unit. Nanosecond transient absorption spectroscopy shows that intramolecular TTET occurred for **69**, since selective photoexcitation into the energy donor (the Bodipy unit) mainly produce the NDI-localized triplet excited state. Intermolecular TTET between **70** and **71** was also studied.<sup>132</sup>

### 2.9. Switchable triplet excited state of broadband visible light-absorbing triplet photosensitizers

Different from the study on *singlet* excited state (such as fluorescence), for which many switching or modulation

mechanisms have been developed,<sup>31</sup> the study on switching of the triplet excited state is rare. Switching of the singlet excited state leads to vast functional molecules, such as fluorescent molecular probes,<sup>31,133</sup> and light-harvesting arrays,<sup>81</sup> etc. Switching of the triplet excited state will also give important compounds such as activatable PDT reagents,<sup>7,134</sup> and molecular machines or logic gates with  $^1\text{O}_2$  as a novel output.<sup>23</sup>

Recently we prepared Bodipy-derived broadband visible light-absorbing triplet photosensitizers which show tunable triplet excited state, either by the solvent polarity or protonation (Fig. 44).<sup>135</sup> In **72**, the Bodipy unit is the singlet energy donor, and the dimethylaminostyrylBodipy is the singlet energy acceptor and the spin converter. In **73**, the uniodinated Bodipy part is the singlet energy acceptor, and the iodinated Bodipy part is the singlet energy donor.

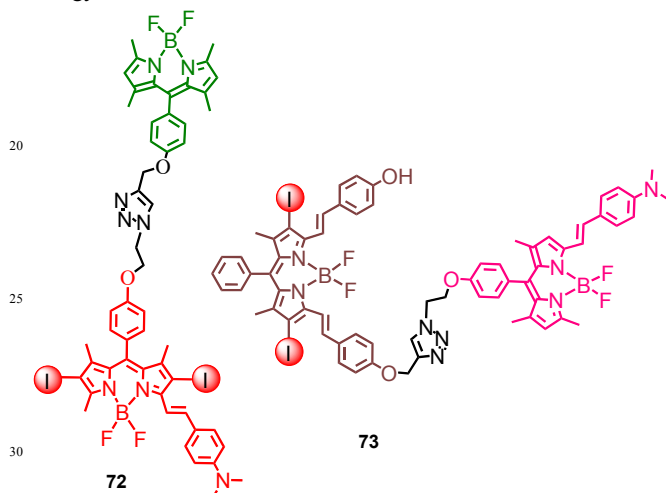


**Fig. 44** Broadband visible light-absorbing Bodipy Dyads (**72** and **73**) with tuneable triplet excited state.<sup>135</sup>

Compound **72** shows strong absorption band at 497 nm and 639 nm due to the uniodinated Bodipy part and the iodinated Bodipy unit (Fig. 45), respectively. For **72** alone, the emission intensity was greatly reduced in polar solvents such as methanol and acetonitrile, compared to that in non-polar solvents such as toluene. Furthermore, the emission wavelength is red-shifted in polar solvents as compared with that in non-polar solvents. These features are typical for the dimethylaminostyrylBodipy.<sup>136</sup> Upon addition of acid such as HCl, the absorption band at 639 nm decreased, a new absorption band at 574 nm was intensified (Fig. 45a). This spectral change is due to the protonation of the aminostyrylBodipy moiety. The fluorescence emission at 594 nm was intensified, without any wavelength changes (Fig. 45b).

For **73**, two absorption bands at 589 nm and 660 nm were observed. The fluorescence emission is center at 693 nm, the emission intensity was decreased in polar solvents. By comparison with the reference compounds, we proved that the emission of **73** is due to the iodinated Bodipy part, the uniodinated Bodipy unit in **73** is the singlet energy acceptor. Hence, **73** is a rare example that the chromophore showing shorter absorption wavelength acts the singlet energy acceptor in the FRET process.<sup>40</sup> This is due to the large Stokes shift of the uniodinated Bodipy part in **73**.

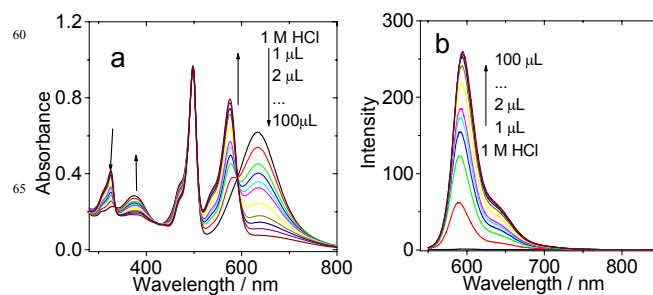


**Fig. 45** Variation of the UV-vis absorption spectra and the fluorescence emission spectra upon protonation with addition of aqueous HCl. (a) Compound **72** with increasing amount of HCl was added and (b) the corresponding emission spectra changes of compound **72** ( $\lambda_{\text{ex}} = 540$  nm) upon addition of the HCl. The aliquots of the HCl solution (1 M) added are 1  $\mu\text{L}$ , 2  $\mu\text{L}$ , 3  $\mu\text{L}$ , 4  $\mu\text{L}$ , 5  $\mu\text{L}$ , 10  $\mu\text{L}$ , 20  $\mu\text{L}$ , 30  $\mu\text{L}$ , 50  $\mu\text{L}$  and 100  $\mu\text{L}$ . In MeCN/H<sub>2</sub>O = 9:1 (v/v), ( $c = 1.0 \times 10^{-5}$  M; 20 °C).<sup>135</sup>

The singlet oxygen ( $^1\text{O}_2$ ) photosensitizing ability of the compounds were evaluated with a  $^1\text{O}_2$  scavenger, 1,3-diphenylisobenzofuran (DPBF). In neutral solution (CH<sub>3</sub>CN:H<sub>2</sub>O 9:1, v/v), no formation of triplet excited state was observed, and the  $^1\text{O}_2$  photosensitizing is negligible ( $\Phi_{\Delta} = 7\%$ ). Upon addition of acid, thus protonation of the amino group, the  $^1\text{O}_2$  photosensitizing quantum yield ( $\Phi_{\Delta}$ ) increased to 73.8%.

Broadband visible light-absorbing C<sub>60</sub>-Bodipy dyads were also prepared for study of the triplet excited state switching (**76** and **77**), **74** and **75** were used as reference compounds (Fig. 46).<sup>137</sup> In these triads, the Bodipy chromophores are the visible light-harvesting antenna and singlet energy donor. C<sub>60</sub> unit is the singlet energy acceptor and the spin converter. Moreover, the Bodipy units are also the electron donor. The visible light-harvesting antenna were selected in such a way that the S<sub>1</sub> state of the styrylBodipy in **75** and **77** is lower than that of C<sub>60</sub>, thus singlet energy transfer from the Bodipy moiety to C<sub>60</sub> is inhibited. On the other hand, singlet energy transfer may occur for **74** and **76**, the triplet state of the dimethylaminostyrylBodipy may be produced by the backward triplet-triplet-energy-transfer (TTET). However, as we discovered earlier, the triplet state of the dimethylaminoStyrylBodipy will be quenched in polar solvents such as dichloromethane. Thus, the triplet state property of the C<sub>60</sub>-Bodipy triads can be switched via a few approaches, such as electron transfer, singlet energy transfer and intra-antenna charge transfer.

For **74**, the absorption band is centered at 622 nm, and the fluorescence emission band is at 660 nm. Thus the S<sub>1</sub> state energy level of the Bodipy antenna in **74** is higher than C<sub>60</sub> (1.75 eV).<sup>78,124</sup> As a result, singlet energy transfer from the Bodipy antenna to C<sub>60</sub> is possible in **74**. Indeed the triplet state of the Bodipy antenna in **74** can be observed in non-polar solvent, such as toluene ( $\tau_{\text{T}} = 168.6$   $\mu\text{s}$ ,  $\Phi_{\Delta} = 1.9\%$ ). But no triplet state was observed for **74** in polar solvents such as dichloromethane. In this case the formation of triplet state is either inhibited by the electron transfer from Bodipy to C<sub>60</sub> or by the intra-antenna charge transfer. Upon addition of TFA, thus protonation of the amino group, the absorption band is blue-shifted to 573 nm, and triplet excited state localized on the Bodipy antenna was observed even in polar solvent (in dichloromethane.  $\tau_{\text{T}} = 4.4$   $\mu\text{s}$ ,  $\Phi_{\Delta} = 73\%$ ).

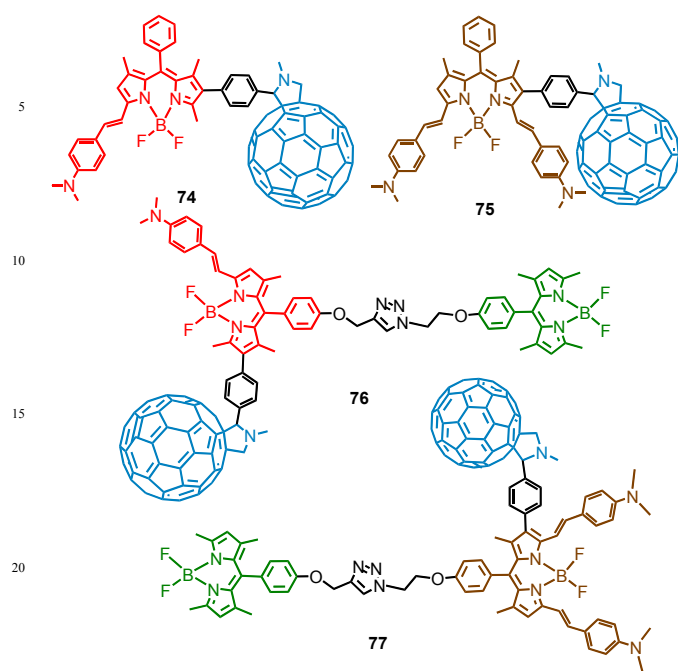


**Fig. 46** Broadband visible light-harvesting  $C_{60}$ -Bodipy triads (**76** and **77**. **74** and **75** are reference compounds).<sup>137</sup>

For **75**, the absorption is at 712 nm, and the fluorescence emission is at 770 nm. Thus the  $S_1$  state energy level of the Bodipy antenna (1.61 eV) is close or lower than that of  $C_{60}$ . Thus singlet energy transfer from the Bodipy antenna to  $C_{60}$  in **75** is inhibited. As a proof of this postulation, no significant formation of triplet excited state was observed for **75**, even in non-polar solvent such as toluene ( $\Phi_{\Delta} = 1.1\%$ ). It is known that photo-induced electron transfer will be inhibited to large extent in nonpolar solvents.<sup>62,124</sup> With addition of TFA, the absorption and fluorescence emission of **75** are blue-shifted to 627 nm and 644 nm, respectively. Thus singlet energy transfer in the protonated **75** become possible. Triplet excited state was observed for **75** upon addition of acid (in dichloromethane.  $\tau_T = 74.8 \mu\text{s}$ ,  $\Phi_{\Delta} = 26\%$ ). Similar results were observed for **76** and **77**, except that broadband visible light absorption was observed for **76** and **77**.

For the above compounds or the broadband visible light-absorbing triplet photosensitizers with triplet state switched, the strong visible light absorption is unable to be switched between the OFF and the ON state. In order to address this challenge, we designed rhodamine- $C_{60}$  dyad **78** and **79** (Fig. 47).<sup>138</sup> The molecular designing rational is that the  $C_{60}$  unit gives weak absorption of visible light, thus in the absence of acid, i.e. with the rhodamine in the spiroactam structure, the dyads show no visible light-absorption. In the presence of acid, the rhodamine unit changed to the opened amide structure, which give strong absorption at 560 nm, thus singlet energy transfer to the  $C_{60}$  unit is activated, the ISC of the  $C_{60}$  will produce the triple state efficiently. The nanosecond transient absorption spectroscopy shows that the production of triplet state is more significant in the presence of acid. The  $^1O_2$  production of the dyads in the absence of acid is negligible. Upon addition of acid, the  $^1O_2$  yield is increased up to 88.5%.

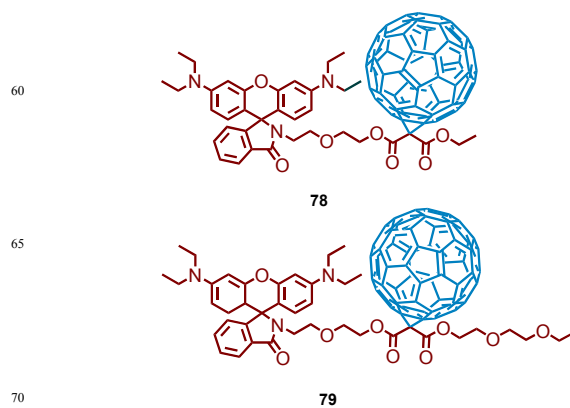


**Fig. 47** Acid-activatable Rhodamine- $C_{60}$  dyad triplet photosensitizers (**78**, **79**).<sup>138</sup>

## 2.10. Broadband visible light-absorbing triplet photosensitizers with competing ISC and FRET

Up to date the molecular structural designing rational of the broadband visible light-absorbing triplet photosensitizers is based on the *desired* profile, i.e. the singlet energy acceptor plays the role of the spin converter. Thus the FRET process is followed by ISC, and this cascade process is beneficial for funneling of the photoexcitation energy for formation of triplet excited state. The alternative profile, i.e. the singlet energy donor as the spin converter, for which a *competing* ISC and FRET will be established, has never been studied. In order to study the photophysics of the broadband visible light-absorbing triplet photosensitizers with competing ISC and FRET, we prepared dyads **82** and triad **83** (Fig. 48),<sup>102</sup> in which competing ISC and FRET is expected.

In **82** and **83**, the iodoBodipy part is the singlet energy donor, and the PBI part is the singlet energy acceptor. Fluorescence of the PBI unit (the singlet energy acceptor) is substantially quenched, thus PET is proposed for the dyad (**82**) and the triad (**83**) photosensitizers. The fluorescence of the diiodoBodipy part is also quenched, thus singlet energy transfer is possible for **82** and **83**. However, PET can not be excluded.<sup>62</sup> We also studied the singlet energy acceptor emission (PBI moiety in **82** and **83**), and the emission was substantially quenched as compared with the reference compounds with phenyl ring attached on the PBI moiety. The results show that the emission of PBI moiety in **82** and **83** were significantly quenched, thus PET is proposed, and it was supported by the calculation of the Gibbs free energy changes ( $\Delta G_{CT}^{\circ}$ ) of the PET process.<sup>62,78,102</sup>

It is known that PBI is with  $T_1$  state energy level of ca. 1.2 eV, which is much lower than Bodipy (ca. 1.69 eV). Thus the  $T_1$  state of the dyad **82** and triad **83** is assumed to be located on the PBI moiety. It should be pointed out that the PBI moiety shows only weak ISC ability, thus significant population of the PBI-localized triplet excited state will indicate intramolecular TTET. The nanosecond transient absorption spectroscopy show that the triplet state of the dyad and triad is localized on the PBI moiety, even with selective photoexcitation into the diiodoBodipy unit (Fig. 49). An exceptionally long-lived triplet excited state lifetime ca. 150  $\mu\text{s}$  was observed (Fig. 49b). Previously with heavy atom effect of Pt(II) the PBI triplet state lifetime was found to be much shorter (less than 1  $\mu\text{s}$ ).<sup>139</sup> The intramolecular TTET process is assumed to be fast because the TTET process

cannot be monitored by the nanosecond transient absorption spectrometer.

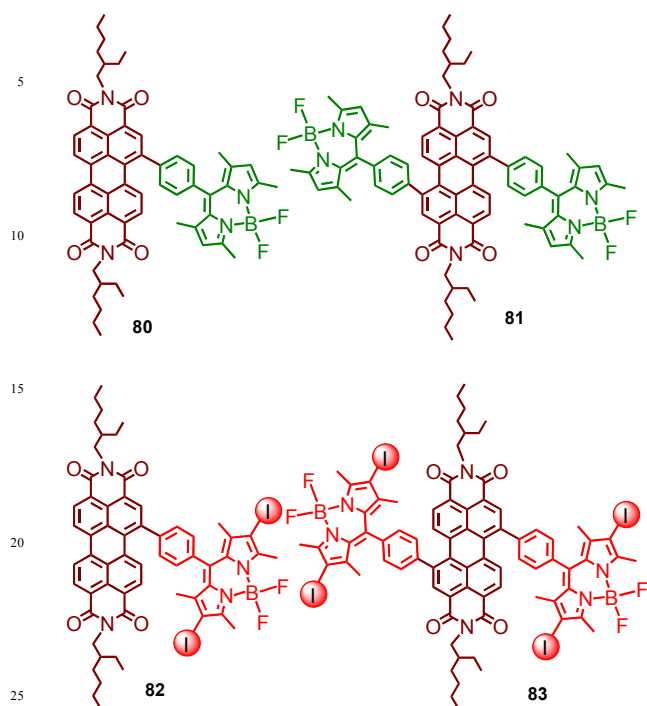


**Fig. 48** Broadband visible light-harvesting PBI-Bodipy dyad **82** and triad **83** with competing ISC and FRET process. Dyad **80** and triad **81** were prepared as reference compounds.<sup>102</sup>

With femtosecond transient absorption spectroscopy, the singlet energy transfer rate constant was determined as  $5 \times 10^{10} \text{ s}^{-1}$ . Previously it was reported that the intersystem crossing rate constants of 2,6-diiodoBodipy is  $7.7 \times 10^9 \text{ s}^{-1}$ .<sup>114</sup> Thus the ISC of the diiodoBodipy moiety should be significantly quenched by the FRET. In other words, the triplet state formation quantum yield ( $\Phi_T$ ) of the dyad **82** and the triad **83** should be low, due to the competition of FRET on the ISC. To our surprise, the triplet state yield of the dyad and the triad (approximated with the singlet oxygen quanaum yield,  $\Phi_\Delta$ ) is high, which were determined as 80% and 78%, respectively. Thus we propose the singlet excited state of the diiodoBodipy in **82** and **83** was trapped somehow, although the faster decay channel of FRET exists.

In order to add modubility to triplet photosensitizers with such novel photophysical properties, we propose that the reversible transformation of rhodamine between the spirolactam and the opened amide structures can be used to switch the triplet excited state as well (Fig. 50).<sup>140</sup> The two structures show drastically different photophysical properties, such as visible light absorption, the  $S_1$  state energy level, as well as  $T_1$  state energy level. The electron donating ability may also change accompanying the spirolactam  $\leftrightarrow$  open amide structure transformation. The spirolactam structure of rhodamine shows no visible light absorption ability, the  $S_1$  state is with high energy level (2.63 eV). The  $T_1$  state energy level is also high (3.36 eV). The electron donating ability is presumably strong. For the opened amide structure, strong absorption at ca. 560 nm emerges, intense fluorescence emission at 580 nm develop, and the  $S_1$  state energy level is ca. 2.13 eV. The  $T_1$  state energy level is 1.73 eV.

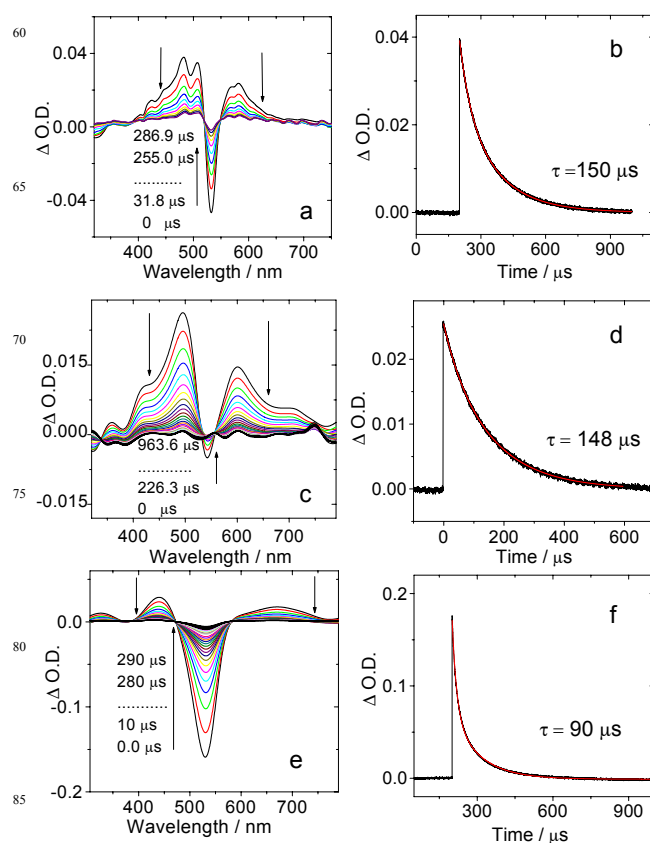


**Fig. 49** Nanosecond transient absorption spectra of **12**, **82** and **83**. (a) Transient absorption spectra of **82** and (b) the decay trace of **82** at 470 nm. (c) Transient absorption difference spectra of **83** and (d) the decay trace of **83** at 470 nm; (e) Transient absorption difference spectra of **12** and (f) Decay trace of **12** at 520 nm.  $\lambda_{\text{ex}} = 532 \text{ nm}$  (nanosecond pulsed laser).  $c = 1.0 \times 10^{-5} \text{ M}$  in deaerated toluene. 20 °C.<sup>102</sup>

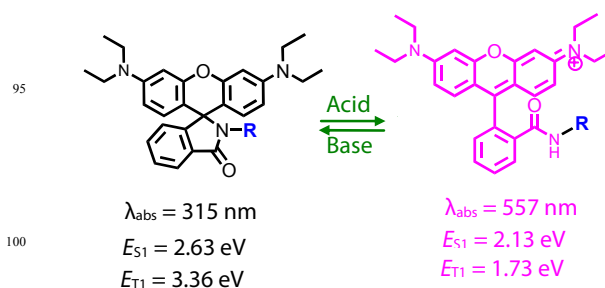


**Fig. 50** Spirolactam-Opened amide structure transformation of Rhodamine.<sup>140</sup>

Based on these spectral property changes, we assume that the spirolactam/opened structural transformation of rhodamine can be used to modulate the triplet excited state of triplet photosensitizers. This structural transformation has been widely used for designing fluorescence molecular chemosensors, i.e. for modulation of singlet excited states,<sup>31,141,142</sup> but it was not used for modulation of triplet excited states. Thus we designed RB-NDI and RB-NI dyads for switching of the triplet excited state (Fig. 51).<sup>140</sup>

In the absence of acid, compound **84** shows a moderate absorption band at 537 nm, which is due to the 2-bromo-6-amino-NDI ( $\epsilon = 10800 \text{ M}^{-1} \text{ cm}^{-1}$ ). The fluorescence of **84** is

weak as compared with that of NDI, thus electron transfer may be responsible for the quenching of the fluorescence of NDI moiety. Upon addition of acid, intense absorption band at 557 nm emerged, which is attributed to the opened amide rhodamine ( $\epsilon = 64400 \text{ M}^{-1} \text{ cm}^{-1}$ ). With optically matched solution, we found that the emission of RB-NDI (**84**)/TFA is half of the emission intensity of RB+TFA. Thus the PET in the RB-NDI (**84**)/TFA is not significant, otherwise the fluorescence of the rhodamine part may be quenched.

No triplet excited state was observed for compound **84** in polar solvents (DCM:MeOH = 9:1, v/v). This lack of the formation of the triplet excited state may be due to the PET in compound **84**, with RB (spirolactam structure) as the electron donor and the NDI part as the electron acceptor, based on the electrochemical property of the compounds.<sup>140</sup>

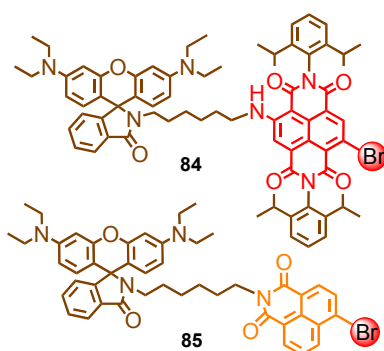


**Fig. 51** Rhodamine-NDI (**84**) and Rhodamine-NI (**85**) dyads showing acid-switchable triplet excited states.<sup>140</sup>

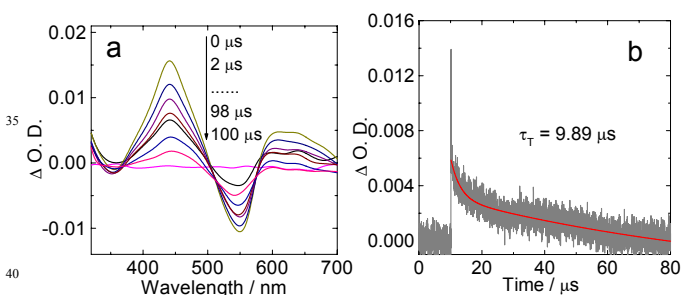


**Fig. 52** Switching the triplet state of compound **84** by addition of TFA. Nanosecond time-resolved transient absorption spectra of (a) **84** in the presence of TFA (100  $\mu\text{L}$ );  $c = 2.0 \times 10^{-5} \text{ M}$ ; (b) decay trace at 450 nm.  $c = 1.0 \times 10^{-5} \text{ M}$ . Excited with 532 nm nanosecond pulsed laser. In deaerated DCM/MeOH (9/1, v/v). 20  $^{\circ}\text{C}$ .<sup>140</sup>

In the presence of acid (TFA), triplet signal was observed for RB-NDI (**84**)+TFA (Fig. 52). The triplet state lifetime was determined as 9.89  $\mu\text{s}$ . The observation of the triplet state is due to the inhibited PET with the rhodamine unit in the opened amide form. By comparison with reference compound, we propose that the triplet state of RB-NDI (**84**)/TFA is delocalized over the RB and the NDI chromophores. This postulation was supported by the TD-DFT computations which show that the dyad is with nearly degenerated  $T_1$  and  $T_2$  states, with a energy gap of only 0.1 eV. The  $T_1$  and  $T_2$  state is confined on the NDI and the rhodamine moieties, respectively. With DPBF as the singlet oxygen ( $^1\text{O}_2$ ) scavenger, we proved that upon addition of acid,

the  $^1\text{O}_2$  quantum yield ( $\Phi_{\Delta}$ ) of RB-NDI increased from 0 to 22%. Similar properties were observed for dyad **85**.

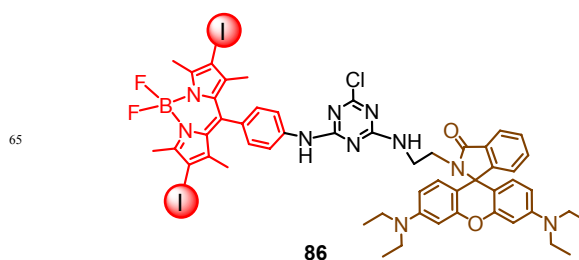


**Fig. 53** DiiodoBodipy-Rhodamine dyad (**86**) with switchable triplet excited state.<sup>103</sup>

We also prepared a diiodoBodipy-Rhodamine dyad **86** (Fig. 53), which is acid-activatable broadband visible light-absorbing dyad (absorption wavelength range 450 – 560 nm).<sup>103</sup> The rhodamine module is transformed to the opened amide form in the presence of acid, thus a acid-activated FRET (with diiodoBodipy module as the singlet energy donor and the rhodamine module as the singlet energy acceptor) will compete with the ISC of the diiodoBodipy module. Given the FRET was faster than the ISC, which was previously proposed for Bodipy dyads, the ISC will be substantially inhibited, thus no triplet excited state formation will be formed for the dyad. With femtosecond transient absorption spectra, we confirmed that the ISC rate constant is  $5.6 \times 10^9 \text{ s}^{-1}$ , the FRET rate constant is  $1.2 \times 10^{10} \text{ s}^{-1}$ . The production of triplet excited state by the dyad is not completely inhibited by the faster, competitive FRET. With nanosecond transient absorption spectroscopy, we confirmed that the triplet excited state confined on the diiodoBodipy unit is produced. The triplet state lifetime is 34.4  $\mu\text{s}$  (in the presence of acid). Based on these conjugates showing competing FRET and ISC, we found that the ISC of the singlet energy donor is unable to be completely quenched by FRET. In some cases, the PET plays the major role for triplet state quenching.

It is still in the very early age for the studying of the broadband visible light-harvesting triplet photosensitizers. Molecular designing strategies for these photosensitizers need to be developed to reduce the synthetic demands, to repress the PET process (clearly this is a undesired side-photophysical process), to ensure efficient FRET and high triplet state yield.

Although there are some reports on preparation of such triplet photosensitizers, the application of these novel compounds is rare. Applications of such photosensitizers in  $^1\text{O}_2$  production and photocatalytic organic reactions were reported, but the enhancement of the photosensitizing efficiency is not always satisfactory. Detail kinetic modeling concerning these photophysical processes will help to elucidate the situation, but at present such studies are left to be done. These studies will be helpful to the areas such as photocatalysis and photovoltaics, as well as fundamental photochemistry studies.

### 3. Conclusion

In summary, the molecular design methods for broadband visible light-absorbing triplet photosensitizers are summarized. Conventional triplet photosensitizers usually contain a single visible light-harvesting chromophore, thus show only a single

major absorption band in visible spectral region, which is a clear disadvantage for harvesting broadband visible light photoexcitation source, such as solar light. Moreover, the single chromophore of the conventional triplet photosensitizers plays the dual-functionality of light-harvesting and intersystem crossing (ISC). Moreover, it is difficult to design heavy atom-free triplet photosensitizers because of the unpredictable ISC of such compounds. In order to address these challenges, application of the Förster-Resonance-Energy-Transfer (FRET) and spin converter leads to a new molecular structure profiles for triplet photosensitizers to attain the broadband visible light-absorption, and to disintegrate the functionality of visible light-harvesting and ISC. New triplet photosensitizers can be easily designed based on the concept of spin converter. This review article summarized the triplet photosensitizers showing broadband visible light absorption. The photophysical processes involved in these multichromophore conjugates, such as the FRET, ISC, the photo-induced electron transfer (PET) studied with nanosecond and femtosecond transient absorption spectroscopy were discussed. The unique photophysical processes, such as the ping-pong energy transfer, and the triplet states equilibrium, were also discussed. The application of the triplet photosensitizers in the areas such as photoredox catalytic organic reactions and triplet-triplet annihilation upconversions were briefly introduced. The remaining challenges in this area include to develop more spin converters, to control the PET process for more efficient triplet state formation, and to apply the broadband visible light-absorbing triplet photosensitizers in photocatalysis and upconversion, etc.

### Acknowledgement

We thank the NSFC (21273028, 21421005 and 21473020), Ministry of Education (SRFDP-20120041130005), Program for Changjiang Scholars and Innovative Research Team in University [IRT\_13R06], State Key Laboratory of Fine Chemicals (KF1203), the Fundamental Research Funds for the Central Universities (DUT14ZD226) and Dalian University of Technology (DUT2013TB07) for financial support.

### Notes and references

State Key Laboratory of Fine Chemicals, School of Chemical Engineering, Dalian University of Technology, E-208 West Campus, 2 Ling-Gong Road, Dalian 116024, P. R. China. E-mail: zhaojzh@dlut.edu.cn Web: <http://finechem2.dlut.edu.cn/photochem>

- 1 A. Kamkaew, S. H. Lim, H. B. Lee, L. V. Kiew, L. Y. Chung and K. Burgess, *Chem. Soc. Rev.*, 2013, **42**, 77–88.
- 2 S. G. Awuah and Y. You, *RSC Adv.*, 2012, **2**, 11169–11183.
- 3 O. J. Stacey and S. J. A. Pope, *RSC Adv.*, 2013, **3**, 25550–25564.
- 4 N. Adarsh, R. R. Avirah and D. Ramaiah, *Org. Lett.*, 2010, **12**, 5720–5723.
- 5 A. Gorman, J. Killoran, C. O'Shea, T. Kenna, W. M. Gallagher and D. F. O'Shea, *J. Am. Chem. Soc.*, 2004, **126**, 10619–10631.
- 6 Y. Cakmak, S. Kolemen, S. Duman, Y. Dede, Y. Dolen, B. Kilic, Z. Kostereli, L. T. Yildirim, A. L. Dogan and D. Guc, *Angew. Chem. Int. Ed.*, 2011, **50**, 11937–11941.
- 7 P. Majumdar, R. Nomula and J. Zhao, *J. Mater. Chem.*, 2014, **2**, 5982–5997.
- 8 J. Zhao, W. Wu, J. Sun and S. Guo, *Chem. Soc. Rev.*, 2013, **42**, 5323–5351.

- 9 J. I. Goldsmith, W. R. Hudson, M. S. Lowry, T. H. Anderson and S. Bernhard, *J. Am. Chem. Soc.*, 2005, **127**, 7502–7510.
- 10 M. Kobayashi, S. Masaoka and K. Sakai, *Angew. Chem. Int. Ed.*, 2012, **51**, 7431–7434.
- 11 B. F. DiSalle and S. Bernhard, *J. Am. Chem. Soc.*, 2011, **133**, 11819–11821.
- 12 F. Gärtner, D. Cozzula, S. Losse, A. Boddien, G. Anilkumar, H. Junge, T. Schulz, N. Marquet, A. Spannenberg and S. Gladioli, *Chem. Eur. J.*, 2011, **17**, 6998–7006.
- 13 L. Shi and W. Xia, *Chem. Soc. Rev.*, 2012, **41**, 7687–7697.
- 14 D. P. Hari and B. König, *Chem. Commun.*, 2014, **50**, 6688–6699.
- 15 C. K. Prier, D. A. Rankic and aa, *Chem. Rev.*, 2013, **113**, 5322–5363.
- 16 D. Ravelli, M. Fagnoni and A. Albini, *Chem. Soc. Rev.*, 2013, **42**, 97–113.
- 17 S. Fukuzumi and K. Ohkubo, *Chem. Sci.*, 2013, **4**, 561–574.
- 18 V. Fernández-Moreira, F. L. Thorp-Greenwood and M. P. Coogan, *Chem. Commun.*, 2010, **46**, 186–202.
- 19 Q. Zhao, F. Li and C. Huang, *Chem. Soc. Rev.*, 2010, **39**, 3007–3030.
- 20 Y. You and W. Nam, *Chem. Soc. Rev.*, 2012, **41**, 7061–7084.
- 21 K. K.-W. Lo, B. T.-N. Chan, H.-W. Liu, K. Y. Zhang, S. P.-Y. Li and T. S.-M. Tang, *Chem. Commun.*, 2013, **49**, 4271–4273.
- 22 K. K. W. Lo, C. K. Chung and N. Zhu, *Chem. Eur. J.*, 2006, **12**, 1500–1512.
- 23 S. Erbas-Cakmak and E. U. Akkaya, *Angew. Chem. Int. Ed.*, 2013, **52**, 11364–11368.
- 24 O. AltanBozdemir, *Chem. Sci.*, 2013, **4**, 858–862.
- 25 T. N. Singh-Rachford and F. N. Castellano, *Coord. Chem. Rev.*, 2010, **254**, 2560–2573.
- 26 J. Zhao, S. Ji and H. Guo, *RSC Adv.*, 2011, **1**, 937–950.
- 27 A. Monguzzi, R. Tubino, S. Hoseinkhani, M. Campione and F. Meinardi, *Phys. Chem. Chem. Phys.*, 2012, **14**, 4322–4332.
- 28 P. Ceroni, *Chem. Eur. J.*, 2011, **17**, 9560–9564.
- 29 Y. C. Simon and C. Weder, *J. Mater. Chem.*, 2012, **22**, 20817–20830.
- 30 J. Zhou, Q. Liu, W. Feng, Y. Sun and F. Li, *Chem. Rev.*, 2015, **115**, 395–465.
- 31 A. P. De Silva, H. Q. N. Gunaratne, T. Gunnlaugsson, A. J. M. Huxley, C. P. McCoy, J. T. Rademacher and T. E. Rice, *Chem. Rev.*, 1997, **97**, 1515–1566.
- 32 (a) H. Lu, J. Mack, Y. Yang and Z. Shen, *Chem. Soc. Rev.*, 2014, **43**, 4778–4823. (b) Y. Chen, C. Zhu, J. Cen, Y. Bai, W. He and Z. Guo, *Chem. Sci.*, 2015, **6**, 3187–3194. (c) Z. Wang, J.-H. Ye, J. Li, Y. Bai, W. Zhang and W. He, *RSC Adv.*, 2015, **5**, 8912–8917. (d) J. Zhang, X.-D. Jiang, X. Shao, J. Zhao, Y. Su, D. Xi, H. Yu, S. Yue, L.-j. Xiao and W. Zhao, *RSC Adv.*, 2014, **4**, 54080–54083.
- 33 (a) X. Chen, Y. Zhou, X. Peng and J. Yoon, *Chem. Soc. Rev.*, 2010, **39**, 2120–2135. (b) S. Lee, K. K. Y. Yuen, K. A. Jolliffe and J. Yoon, *Chem. Soc. Rev.*, 2015, **44**, 1749–1762. (c) A. Dvivedi, P. Rajakannu and M. Ravikanth, *Dalton Trans.*, 2015, **44**, 4054–4062. (d) S. Madhu, S. Josimuddin and M. Ravikanth, *New J. Chem.*, 2014, **38**, 3770–3776. (e) D.-T. Shi, D. Zhou, Y. Zang, J. Li, G.-R. Chen, T. D. James, X.-P. He and H. Tian, *Chem. Commun.*, 2015, **51**, 3653–3655. (f) M. Li, Z. Guo, W. Zhu, F. Marken and T. D. James, *Chem. Commun.*, 2015, **51**, 1293–1296. (g) Y. Cao, L. Ding, W. Hu, J. Peng and Y. Fang, *J. Mater. Chem. A*, 2014, **2**, 18488–18496.
- 34 P.-T. Chou, Y. Chi, M.-W. Chung and C.-C. Lin, *Coord. Chem. Rev.*, 2011, **255**, 2653–2665.
- 35 S. C. Chan, M. C. W. Chan, Y. Wang, C. M. Che, K. K. Cheung and N. Zhu, *Chem. Eur. J.*, 2001, **7**, 4180–4190.
- 36 S. Y. L. Leung, E. S. H. Lam, W. H. Lam, K. M. C. Wong, W. T. Wong and V. W. W. Yam, *Chem. Eur. J.*, 2013, **19**, 10360–10369.
- 37 T. Peng, Y. Yang, Y. Liu, D. Ma, Z. Hou and Y. Wang, *Chem. Commun.*, 2011, **47**, 3150–3152.
- 38 Q. Liu, L. Thorne, I. Kozin, D. Song, C. Seward, M. D'Iorio, Y. Tao and S. Wang, *J. Chem. Soc., Dalton Trans.*, 2002, 3234–3240.
- 39 Y. Kang, Y.-L. Chang, J.-S. Lu, S.-B. Ko, Y. Rao, M. Varlan, Z.-H. Lu and S. Wang, *J. Mater. Chem. C*, 2013, **1**, 441–450.
- 40 J. R. Lakowicz, *Principles of Fluorescence Spectroscopy*, 2nd ed.; Kluwer Academic/Plenum Publishers: New York, 1999.
- 41 S. Ji, W. Wu, W. Wu, H. Guo and J. Zhao, *Angew. Chem. Int. Ed.*, 2011, **50**, 1626–1629.

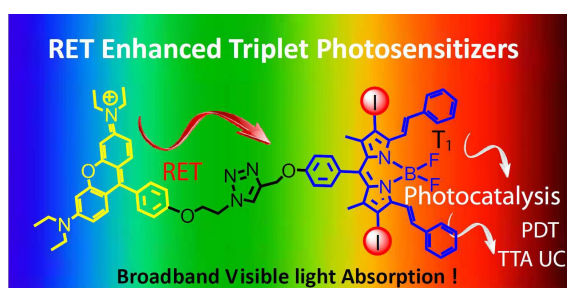
- 42 H. Xiang, J. Cheng, X. Ma, X. Zhou and J. J. Chruma, *Chem. Soc. Rev.*, 2013, **42**, 6128–6185.
- 43 J. Zhao, S. Ji, W. Wu, W. Wu, H. Guo, J. Sun, H. Sun, Y. Liu, Q. Li and L. Huang, *RSC Adv.*, 2012, **2**, 1712–1728.
- 44 M. Schulze, A. Steffen and F. Würthner, *Angew. Chem. Int. Ed.*, 2015, **54**, 1570–1573.
- 45 N. Adarsh, M. Shanmugasundaram, R. R. Avirah and D. Ramaiah, *Chem. Eur. J.*, 2012, **18**, 12655–12662.
- 46 W. Wu, J. Zhao, J. Sun and S. Guo, *J. Org. Chem.*, 2012, **77**, 5305–5312.
- 47 Z. Qiao, H. Liu, X. Xiao, Y. Fu, J. Wei, Y. Li and X. Jiang, *Org. Lett.*, 2013, **15**, 2594–2597.
- 48 L. Huang, X. Cui, B. Therrien and J. Zhao, *Chem. Eur. J.*, 2013, **19**, 17472–17482.
- 49 S. Campagna, F. Puntoriero, F. Nastasi, G. Bergamini and V. Balzani, in *Photochemistry and Photophysics of Coordination Compounds I*, Springer, 2007, **280**, 117–214.
- 50 R. Lincoln, L. Kohler, S. Monro, H. Yin, M. Stephenson, R. Zong, A. Chouai, C. Dorsey, R. Hennig and R. P. Thummel, *J. Am. Chem. Soc.*, 2013, **135**, 17161–17175.
- 51 Y. Q. Zou, L. Q. Lu, L. Fu, N. J. Chang, J. Rong, J. R. Chen and W. J. Xiao, *Angew. Chem. Int. Ed.*, 2011, **50**, 7171–7175.
- 52 S. Sato, T. Morikawa, T. Kajino and O. Ishitani, *Angew. Chem. Int. Ed.*, 2013, **52**, 988–992.
- 53 Q. Liu, Y. N. Li, H. H. Zhang, B. Chen, C. H. Tung and L. Z. Wu, *Chem. Eur. J.*, 2012, **18**, 620–627.
- 54 X. Gu, X. Li, Y. Chai, Q. Yang, P. Li and Y. Yao, *Green Chem.*, 2013, **15**, 357–361.
- 55 D. Kalaitzakis, T. Montagnon, I. Alexopoulou and G. Vassilikogiannakis, *Angew. Chem. Int. Ed.*, 2012, **51**, 8868–8871.
- 56 C. Zhang, J. Zhao, S. Wu, Z. Wang, W. Wu, J. Ma, S. Guo and L. Huang, *J. Am. Chem. Soc.*, 2013, **135**, 10566–10578.
- 57 J. Ma, X. Yuan, B. Küçüköz, S. Li, C. Zhang, P. Majumdar, A. Karatay, X. Li, H. G. Yaglioglu and A. Elmali, *J. Mater. Chem. C*, 2014, **2**, 3900–3913.
- 58 S. Guo, L. Ma, J. Zhao, B. Küçüköz, A. Karatay, M. Hayvali, H. G. Yaglioglu and A. Elmali, *Chem. Sci.*, 2014, **5**, 489–500.
- 59 A. Harriman, M. A. H. Alamiry, J. P. Hagon, D. Hablot and R. Ziessel, *Angew. Chem. Int. Ed.*, 2013, **52**, 6611–6615.
- 60 R. Guliyev, A. Coskun and E. U. Akkaya, *J. Am. Chem. Soc.*, 2009, **131**, 9007–9013.
- 61 X. Zhang, Y. Xiao and X. Qian, *Org. Lett.*, 2008, **10**, 29–32.
- 62 M. E. El - Khouly, A. N. Amin, M. E. Zandler, S. Fukuzumi and F. D'Souza, *Chem. Eur. J.*, 2012, **18**, 5239–5247.
- 63 (a) T. Lazarides, G. Charalambidis, A. Vuillamy, M. Réglie, E. Klontzas, G. Froudakis, S. Kuhri, D. M. Guldi and A. G. Coutsolelos, *Inorg. Chem.*, 2011, **50**, 8926–8936. (b) X. Zhou, X. Wu and J. Yoon, *Chem. Commun.*, 2015, **51**, 111–113.
- 64 H. Jia, B. Küçüköz, Y. Xing, P. Majumdar, C. Zhang, A. Karatay, G. Yaglioglu, A. Elmali, J. Zhao and M. Hayvali, *J. Mater. Chem. C*, 2014, **2**, 9720–9736.
- 65 M. T. Whited, P. I. Djurovich, S. T. Roberts, A. C. Durrell, C. W. Schlenker, S. E. Bradforth and M. E. Thompson, *J. Am. Chem. Soc.*, 2011, **133**, 88–96.
- 66 F. Li, S. I. Yang, Y. Ciringh, J. Seth, C. H. Martin, D. L. Singh, D. Kim, R. R. Birge, D. F. Bocian and D. Holten, *J. Am. Chem. Soc.*, 1998, **120**, 10001–10017.
- 67 N. J. Turro, V. Ramamurthy, J. C. Scaiano, *Principles of Molecular Photochemistry: An Introduction*; University Science Books: Sausalito, CA, 2009.
- 68 M. K. Kuimova, G. Yahioglu, J. A. Levitt and K. Suhling, *J. Am. Chem. Soc.*, 2008, **130**, 6672–6673.
- 69 L. Wang, Y. Xiao, W. Tian, and L. Deng, *J. Am. Chem. Soc.*, 2013, **135**, 2903–2906.
- 70 A. Loudet and K. Burgess, *Chem. Rev.*, 2007, **107**, 4891–4932.
- 71 G. Ulrich, R. Ziessel and A. Harriman, *Angew. Chem. Int. Ed.*, 2008, **47**, 1184–1201.
- 72 X. Yu, X. Jia, X. Yang, W. Liu and W. Qin, *RSC Adv.*, 2014, **4**, 23571–23579.
- 73 J.-H. Ye, J. Xu, H. Chen, Y. Bai, W. Zhang and W. He, *RSC Adv.*, 2014, **4**, 6691–6695.
- 74 R. Bandichhor, A. D. Petrescu, A. Vespa, A. B. Kier, F. Schroeder and K. Burgess, *J. Am. Chem. Soc.*, 2006, **128**, 10688–10689.
- 75 C. W. Wan, A. Burghart, J. Chen, F. Bergström, L. B. Å. Johansson, M. F. Wolford, T. G. Kim, M. R. Topp, R. M. Hochstrasser and K. Burgess, *Chem. Eur. J.*, 2003, **9**, 4430–4441.
- 76 S. Perun, J. Tatchen and C. M. Marian, *ChemPhysChem*, 2008, **9**, 282–292.
- 77 M. Pineiro, A. L. Carvalho, M. M. Pereira, A. M. d. A. Gonsalves, L. G. Arnaut and S. J. Formosinho, *Chem. Eur. J.*, 1998, **4**, 2299–2307.
- 78 R. Ziessel, B. D. Allen, D. B. Rewinska and A. Harriman, *Chem. Eur. J.*, 2009, **15**, 7382–7393.
- 79 J.-Y. Liu, M. E. El-Khouly, S. Fukuzumi and D. K. Ng, *Chem. Asian J.*, 2011, **6**, 174–179.
- 80 Z. Kostereli, T. Ozdemir, O. Buyukcakil and E. U. Akkaya, *Org. Lett.*, 2012, **14**, 3636–3639.
- 81 R. Ziessel and A. Harriman, *Chem. Commun.*, 2011, **47**, 611–631.
- 82 J. Fan, M. Hu, P. Zhan and X. Peng, *Chem. Soc. Rev.*, 2013, **42**, 29–43.
- 83 J.-Y. Liu, Y. Huang, R. Menting, B. Röder, E. A. Ermilov and D. K. P. Ng, *Chem. Commun.*, 2013, **49**, 2998–3000.
- 84 V. Engelhardt, S. Kuhri, J. Fleischhauer and M. Garcia-Iglesias, *Chem. Sci.*, 2013, **4**, 3888–3893.
- 85 A. C. Benniston and G. Copley, *Phys. Chem. Chem. Phys.*, 2009, **11**, 4124–4131.
- 86 T. Lazarides, T. M. McCormick, K. C. Wilson, S. Lee, D. W. McCamant and R. Eisenberg, *J. Am. Chem. Soc.*, 2010, **133**, 350–364.
- 87 R. P. Sabatini, B. Zheng, W. Fu, D. J. Mark, M. F. Mark, E. A. Hillenbrand, R. Eisenberg and D. W. McCamant, *J. Phys. Chem. A*, 2014, **118**, 10663–10672.
- 88 Z. E. X. Dance, S. M. Mickleby, T. M. Wilson, A. B. Ricks, A. M. Scott, M. A. Ratner and M. R. Wasielewski, *J. Phys. Chem. A*, 2008, **112**, 4194–4201.
- 89 J. Y. Liu, M. E. El - Khouly, S. Fukuzumi and D. K. P. Ng, *Chem. Eur. J.*, 2011, **17**, 1605–1613.
- 90 S. Suzuki, R. Sugimura, M. Kozaki, K. Keyaki, K. Nozaki, N. Ikeda, K. Akiyama and K. Okada, *J. Am. Chem. Soc.*, 2009, **131**, 10374–10375.
- 91 W. J. Shi, M. E. El-Khouly, K. Ohkubo, S. Fukuzumi and D. K. P. Ng, *Chem. Eur. J.*, 2013, **19**, 11332–11341.
- 92 V. M. Blas-Ferrando, J. Ortiz, K. Ohkubo, S. Fukuzumi, F. Fernández-Lázaro and Á. Sastre-Santos, *Chem. Sci.*, 2014, **5**, 4785–4793.
- 93 J. J. Apperloo, C. Martineau, P. A. van Hal, J. Roncali and R. A. J. Janssen, *J. Phys. Chem. A*, 2002, **106**, 21–31.
- 94 F. Scarel, C. Ehli, D. M. Guldi and A. Mateo-Alonso, *Chem. Commun.*, 2013, **49**, 9452–9454.
- 95 Y. Han, L. Dobeck, A. Gong, F. Meng, C. W. Spangler and L. H. Spangler, *Chem. Commun.*, 2005, 1067–1069.
- 96 W.-J. Shi, R. Menting, E. A. Ermilov, P.-C. Lo, B. Röder and D. K. P. Ng, *Chem. Commun.*, 2013, **49**, 5277–5279.
- 97 G. N. Lim, E. Maligaspe, M. E. Zandler and F. D'Souza, *Chem. Eur. J.*, 2014, **20**, 17089–17099.
- 98 T. Lazarides, S. Kuhri, G. Charalambidis, M. K. Panda, D. M. Guldi and A. G. Coutsolelos, *Inorg. Chem.*, 2012, **51**, 4193–4204.
- 99 J.-Y. Liu, H.-S. Yeung, W. Xu, X. Li and D. K. P. Ng, *Org. Lett.*, 2008, **10**, 5421–5424.
- 100 C. G. Claessens, D. González-Rodríguez and T. Torres, *Chem. Rev.*, 2002, **102**, 835–853.
- 101 S. Yamauchi, A. Takahashi, Y. Iwasaki, M. Unno, Y. Ohba, J. Higuchi, A. Blank and H. Levanon, *J. Phys. Chem. A*, 2003, **107**, 1478–1485.
- 102 Z. Mahmood, K. Xu, B. Küçüköz, X. Cui, J. Zhao, Z. Wang, A. Karatay, H. G. Yaglioglu, M. Hayvali and A. Elmali, *J. Org. Chem.*, 2015, **80**, 3036–3049.
- 103 K. Xu, Y. Xie, X. Cui, J. Zhao and K. D. Glusac, *J. Phys. Chem. B*, 2015, **119**, 4175–4187.
- 104 J.-Y. Liu, E. A. Ermilov, B. Röder and D. K. P. Ng, *Chem. Commun.*, 2009, 1517–1519.
- 105 E. A. Ermilov, J.-Y. Liu, D. K. P. Ng and B. Röder, *Phys. Chem. Chem. Phys.*, 2009, **11**, 6430–6440.
- 106 W. Chidawanyika and T. Nyokong, *J. Photochem. Photobiol. A*, 2009, **206**, 169–176.

- 107 P. Khoza, E. Antunes and T. Nyokong, *Polyhedron*, 2013, **61**, 119–125.
- 108 A. Barbon, M. Brustolon and E. E. van Faassen, *Phys. Chem. Chem. Phys.*, 2001, **3**, 5342–5347.
- 5 109 C. B. Kc, G. N. Lim, P. A. Karr and F. D'Souza, *Chem. Eur. J.*, 2014, **20**, 7725–7735.
- 110 J. Shao, H. Sun, H. Guo, S. Ji, J. Zhao, W. Wu, X. Yuan, C. Zhang and T. D. James, *Chem. Sci.*, 2012, **3**, 1049–1061.
- 111 X. Zhang, Y. Xiao, and X. Qian, *Angew. Chem. Int. Ed.*, 2008, **47**, 8025–8029.
- 10 112 T. Yogo, Y. Urano, Y. Ishitsuka, F. Maniwa and T. Nagano, *J. Am. Chem. Soc.*, 2005, **127**, 12162–12163.
- 113 W. Wu, H. Guo, W. Wu, S. Ji and J. Zhao, *J. Org. Chem.*, 2011, **76**, 7056–7064.
- 15 114 R. P. Sabatini, T. M. McCormick, T. Lazarides, K. C. Wilson, R. Eisenberg and D. W. McCamant, *J. Phys. Chem. Lett.*, 2011, **2**, 223–227.
- 115 P. Batat, M. Cantuel, G. Jonusauskas, L. Scarpantonio, A. Palma, D. F. O'Shea and N. D. McClenaghan, *J. Phys. Chem. A*, 2011, **115**, 14034–14039.
- 20 116 J. E. Yarnell, J. C. Deaton, C. E. McCusker and F. N. Castellano, *Inorg. Chem.*, 2011, **50**, 7820–7830.
- 117 A. D. Quartarolo, N. Russo and E. Sicilia, *Chem. Eur. J.*, 2006, **12**, 6797–6803.
- 25 118 A. A. Rachford, R. Ziessel, T. Bura, P. Retailleau and F. N. Castellano, *Inorg. Chem.*, 2010, **49**, 3730–3736.
- 119 W. Wu, J. Zhao, H. Guo, J. Sun, S. Ji and Z. Wang, *Chem. Eur. J.*, 2012, **18**, 1961–1968.
- 120 Y. Liu, X. Lv, Y. Zhao, J. Liu, Y.-Q. Sun, P. Wang and W. Guo, *J. Mater. Chem.*, 2012, **22**, 1747–1750.
- 30 121 R. He, M. Hu, T. Xu, C. Li, C. Wu, X. Guo and Y. Zhao, *J. Mater. Chem. C*, 2015, **3**, 973–976.
- 122 A. N. Amin, M. E. El-Khouly, N. K. Subbaiyan, M. E. Zandler, S. Fukuzumi and F. D'Souza, *Chem. Commun.*, 2012, **48**, 206–208.
- 35 123 C. C. Hofmann, S. M. Lindner, M. Ruppert, A. Hirsch, S. A. Haque, M. Thelakkat and J. Köhler, *J. Phys. Chem. B*, 2010, **114**, 9148–9156.
- 124 J. W. Arbogast, A. P. Darmanyan, C. S. Foote, F. N. Diederich, R. L. Whetten, Y. Rubin, M. M. Alvarez and S. J. Anz, *J. Phys. Chem.*, 1991, **95**, 11–12.
- 40 125 S. Guo, J. Sun, L. Ma, W. You, P. Yang and J. Zhao, *Dyes. Pigm.*, 2013, **96**, 449–458.
- 126 D. Huang, J. Zhao, W. Wu, X. Yi, P. Yang and J. Ma, *Asian J. Org. Chem.*, 2012, **1**, 264–273.
- 127 W. Y. Wong and P. D. Harvey, *Macromol. Rapid Commun.* 2010, **31**, 671–713.
- 45 128 C. K. M. Chan, C.-H. Tao, K.-F. Li, K. M.-C. Wong, N. Zhu, K.-W. Cheah and V. W.-W. Yam, *Dalton Trans.*, 2011, **40**, 10670–10685.
- 129 Y. Li, R. W. Winkel, N. Weisbach, J. A. Gladysz and K. S. Schanze, *J. Phys. Chem. A*, 2014, **118**, 10333–10339.
- 50 130 K. S. Schanze, E. E. Silverman and X. Zhao, *J. Phys. Chem. B*, 2005, **109**, 18451–18459.
- 131 W. Wu, J. Zhao, J. Sun, L. Huang and X. Yi, *J. Mater. Chem. C*, 2013, **1**, 705–716.
- 132 L. Liu, S. Guo, J. Ma, K. Xu, J. Zhao and T. Zhang, *Chem. Eur. J.*, 2014, **20**, 14282–14295.
- 55 133 Y. Ding, Y. Tang, W. Zhu and Y. Xie, *Chem. Soc. Rev.*, 2015, **44**, 1101–1112.
- 134 J. Tian, L. Ding, H. Xu, Z. Shen, H. Ju, L. Jia, L. Bao and J. Yu, *J. Am. Chem. Soc.*, 2013, **135**, 18850–18858.
- 60 135 L. Huang, W. Yang and J. Zhao, *J. Org. Chem.*, 2014, **79**, 10240–10255.
- 136 M. Baruah, W. Qin, C. Flors, J. Hofkens, R. A. L. Vallée, D. Beljonne, M. Van der Auweraer, W. M. De Borggraeve and N. Boens, *J. Phys. Chem. A*, 2006, **110**, 5998–6009.
- 65 137 L. Huang and J. Zhao, *J. Mater. Chem. C*, 2015, **3**, 538–550.
- 138 F. Wang, X. Cui, Z. Lou, J. Zhao, M. Bao and X. Li, *Chem. Commun.*, 2014, **50**, 15627–15630.
- 139 A. A. Rachford, S. Goeb and F. N. Castellano, *J. Am. Chem. Soc.*, 2008, **130**, 2766–2767.
- 70 140 X. Cui, J. Zhao, Z. Lou, S. Li, H. Wu and K.-I. Han, *J. Org. Chem.*, 2015, **80**, 568–581.
- 141 L. Yuan, W. Lin, K. Zheng, L. He and W. Huang, *Chem. Soc. Rev.*, 2013, **42**, 622–661.
- 142 B. Zou, H. Liu, J. Mack, S. Wang, J. Tian, H. Lu, Z. Li and Z. Shen, *RSC Adv.*, 2014, **4**, 53864–53869.

Graphical Abstract:

**Application of singlet energy transfer in triplet state formation: broadband visible light-absorbing triplet photosensitizers, molecular structure design, related photophysics and applications**

Xiaoneng Cui, Caishun Zhang and Kejing Xu and Jianzhang Zhao\*



The molecular structure designing, photophysical properties and the application of the broadband visible light-absorbing triplet photosensitizers were summarized.